Master's thesis

NTNU
Norwegian University of Science and Technology
Faculty of Engineering
Department of Marine Technology

Jonas Vørrang Jam

Buckling strength analysis of aluminium plates with varying panel thickness and heat-affected zone patterns

Master's thesis in Marine Structures
Supervisor: Jørgen Amdahl
February 2021

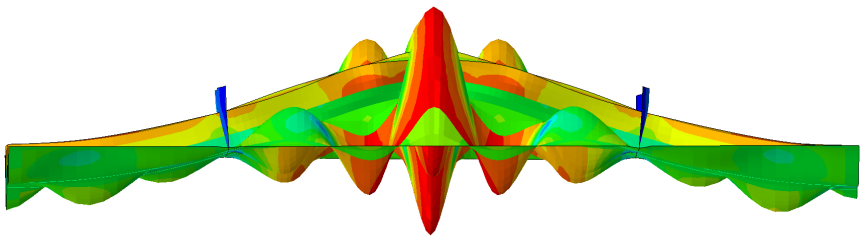

NTNU
Kunnskap for en bedre verden

Jonas Vørrang Jam

Buckling strength analysis of aluminium plates with varying panel thickness and heat-affected zone patterns

Master's thesis in Marine Structures
Supervisor: Jørgen Amdahl
February 2021

Norwegian University of Science and Technology
Faculty of Engineering
Department of Marine Technology

NTNU
Norwegian University of
Science and Technology

Abstract

Aluminium is a material that has many valuable properties the shipping industry can benefit from. For one, its high specific strength has targeted it as a prime candidate as a building material for high speed and light crafts resulting in decreased greenhouse emissions compared to steel-hull boats. Aluminium hulls can also be cheaper to maintain as some aluminium alloys are highly corrosion resistant. However, aluminium is much less studied than steel and has some weaknesses that need to be considered. For one, the heat-affected zones around large welds can have over a 50% reduction in proof strength. Also, aluminium has lower stiffness and is, therefore, more prone to buckling than, for example, steel.

This thesis aimed to study the effect of dimension thickness and weld reduction on stiffened aluminium panels. A parameter study of the buckling load was conducted in Abaqus, and the results were evaluated and compared with *Eurocode 9* and DNV GLs *RU-HSLC*. In summary, the buckling strength of 7 aluminium panels with varying thickness and 6 panels with varying patterns of the heat-affected zones were analysed. The plate thickness varied between 5-6 mm, the step and flange thickness varied between 5-8 mm, and the transverse girder thickness varied between 8-10 mm.

The buckling load analysis indicated that the longitudinal weld zones gave a huge reduction in buckling strength. Contrasting, the transverse weld zones with lateral support had a negligible effect. Plates with no weld zones at all increased their buckling capacity by $\sim$ 19% , while those with only one weld zone had an increase of 12%. Changes in panel thicknesses generally had a smaller effect than changing the heat-affected zone pattern. An increase in plate thickness from 6 to 7 mm had the most considerable effect with an increase in buckling load of $\sim$ 5.6%. The effect of changing the panel thickness was approximately linear with the cross-sectional area, and thus its weight.

These results indicate that the heat-affected zone and the panel dimensions significantly impact the buckling load. Increasing the knowledge on aluminium wielding properties can result in lower margins of the wielding zone's reduction and extent. This information can further result in the production of even lighter and faster ship hulls.

Sammendrag

Aluminium er ett materiale med mange verdifulle egenskaper industrien kan dra nytte av. Dets høye spesifikke styrke gjør det til en ypperlig kandidat til å bygge lette skrog til hurtiggående båter med lavere klima utslipp enn tilsvarende stålbåter. Aluminiumsskrog kan også være billige å vedlikeholde, da enkelte aluminiums legeringer er svært korrosjonsresistente.

Men, aluminium er mindre studert enn stål og har enkelte svakheter som må tas hensyn til. Styrkereduksjon i varmepåvirket sone rundt sveiser kan være over 50% for enkelte legeringer. Aluminium har også lavere stivhet og er dermed mer utsatt for knekking enn stål.

Hensikten med denne oppgaven var å studere effekten av dimensjonstykkelser og sveisereduksjon for en avstivet aluminiums plate. Det ble utført en parameterstudie av knekklasten til ett aluminiumspanel i Abaqus og resultatet ble evaluert og sammenlignet med *Eurocode 9* og DNVGLs *RU-HSLC*.

Totalt ble knekkstyrken til 7 aluminimumspanel med ulike tykkelser og 6 aluminiumspanel med ulike mønstere av varmepåvirket sone analysert. Platetykkelsen varierte mellom 5 mm og 6 mm, stegtykkelsen og flenstykkelsen varierte fra 5 mm til 8 mm og tverrammetykkelsen varierte fra 8 mm til 10 mm.

Knekkanalysen viste at langsgående sveisesoner ga stor reduksjon i knekkstyrke, men at tversgående sveisesoner med lateral støtte har neglisjerbar effekt. Uten noen sveisesoner ble knekklasten økt med $\sim$ 19%, mens dersom det kun var sveisesone på steget økte knekklasten med 12%.

Endring av paneltykkelsene hadde generelt mindre effekt, enn endring av mønsteret til sveisesonen. Endring av platetykkelse fra 6 mm til 7 mm størst effekt med en økning i knekklast på $\sim$ 5.6%. Effekten av endret paneltykkelse var også tilnærmet lineær med endring av panelts tverrsnittsareal, og dermed også vekt.

Disse resultatene indikerer at sveisesonen og paneldimensjonene har stor påvirkning på knekklasten. Dersom man kjenner sveiseegenskapene bedre kan man ha lavere marginer når det kommer til reduksjonsgrad og bredden til sveisesonen. Da kan man produsere enda lettere og raskere skipsskrog.

Acknowledgments

This master thesis was written at the Department of Marine Technology, Norwegian University of Science and Technology. It concludes my Master of Science in Marine Structures and starts a new chapter of my life.

Foremost, I would like to express my sincere gratitude to my supervisor Prof. Jørgen Amdahl for the continuous support, patience and valuable help throughout this work. I want to thank Tord Hansen Kaasa for being co-advisor of the literature study precluding this thesis.

I want to thank my parents Unni and Mansor for encouraging me throughout my studies, for guiding me through 13 years of schooling and always caring for me. Thanks to my brother Kasper and my cousin Marius and the rest of my family.

Thanks to my friends who have given me many memorable moments and have made my studies in Trondheim the best time of my life, so far.

From the bottom of my heart, I want to thank my girlfriend Madeleine, for her love, patience and encouragement. Thanks for proofreading my thesis, for helping me with R, for valuable writing guidance, for making my stressful days easier and for brightening up my day, every single one.

Jonas Vørrang Jam
February 2021

Contents

Abstract . . . . . **iii**
Sammendrag . . . . . **iv**
Acknowledgments . . . . . **v**
Contents . . . . . **vi**
Figures . . . . . **ix**
Tables . . . . . **xi**
Nomenclature . . . . . **xiii**
1 Introduction **1**
1.1 Scope 1
2 Aluminium as Structural Material **4**
2.1 Introduction of Aluminium Properties 4
2.2 Aluminium Alloys and Tempers 5
2.3 The 5xxx Alloy Series 5
2.4 The 6xxx Alloy Series 6
2.5 Residual Stresses and Distortions 6
2.6 Heat affected Zone 8
2.7 Welding Methods 8
2.8 Ramberg-Osgood 9
3 Panel Buckling Theory **11**
3.1 Buckling Intro 11
3.2 The slenderness Parameter 12
3.3 Buckling of Initially Perfect Plates 13
3.4 The Effective Thickness Method 14
3.5 Models for Buckling of Stiffened Plates 15
3.6 The Effective Width Method 17
3.7 Residual Stresses 17
4 Review of Eurocode 9 and HSLC **19**
4.1 Background 19
4.1.1 Limit State Design 19
4.2 Intro to Eurocode 21
4.3 Aluminium Properties in Eurocode 9 21
4.3.1 Alloy Selection for Panel Buckling 21
4.4 Buckling Resistance of Members According to Eurocode 9 22
4.4.1 Material Buckling Class 23

4.4.2 HAZ softening adjacent to welds . . . 23
4.4.3 Cross-Section Class . . . 24
4.4.4 Computing cross-section resistance . . . 24
4.5 Estimation of Panel Buckling Resistance . . . 25
4.5.1 Stiffened Panel under Uniform Compression . . . 25
4.5.2 Plate under Uniform Compression . . . 26
4.5.3 Resistance Under Combined Loading . . . 27
4.6 DNV GL's RU-HSLC . . . 27
4.6.1 Class notations in brief . . . 27
4.6.2 Aluminium Material Properties in HSLC . . . 28
4.6.3 Allowable stresses . . . 28
4.7 Design Loads . . . 28
4.7.1 Slamming Pressure on Bottom . . . 29
4.7.2 Pitching Slamming Pressure on Bottom . . . 29
4.7.3 Longitudinal and Transverse Loads . . . 31
4.8 Structural Requirements . . . 32
4.8.1 DNV GL Buckling Regulation . . . 34
4.8.2 Elastic Buckling of Stiffened Panels . . . 35
4.9 HSLC Uni-axial Compression Buckling . . . 35
5 Abaqus and Finite Element Theory . . . 37
5.1 Nonlinear Finite Element Method . . . 37
5.1.1 Linear and nonlinear analysis . . . 37
5.2 Material Nonlinearity . . . 38
5.3 Geometrical Nonlinearity . . . 38
5.3.1 True strain-stress relations . . . 38
5.4 Abaqus . . . 39
5.4.1 Elements . . . 39
5.5 Linear Eigenvalue Buckling Analysis by Abaqus . . . 40
5.6 Riks Method . . . 41
5.6.1 The Modified Riks Method by Abaqus . . . 41
6 Method - Ultimate Buckling Strength of a Stiffened Panel . . . 43
6.1 Assembly and Dimensions . . . 44
6.2 Material data and HAZ . . . 44
6.3 Meshing and Element types . . . 46
6.3.1 Panel Mesh . . . 46
6.3.2 Girder Mesh . . . 47
6.4 Boundary Conditions and Constraints . . . 47
6.5 Load Conditions . . . 49
6.6 Imperfections . . . 49
6.7 Riks Analysis . . . 50
7 Results . . . 56
7.1 Abaqus - Results . . . 56
7.1.1 Change of Dimensions . . . 56
7.1.2 Abaqus - Change of HAZ Patterns . . . 57

7.1.3 Change of Poisson's Ratio 57
7.2 Results table 58
7.2.1 Correlation of Area and ULS 58
7.3 Eurocode 9 Results 59
8 Discussion 66
8.0.1 Abaqus Results versus Eurocode 9 66
8.1 Changing the HAZ Pattern 66
8.1.1 Change of Poisson's Ratio 66
8.1.2 Unstiffened Panel Model 67
8.1.3 Correlation between Area and ULS 67
8.2 Potential Sources of Modelling Errors 68
9 Conclusion 70
Bibliography 71

Figures

2.1 Residual stresses induced by welding [15]. 7
2.2 Residual stresses induced by rolling [10]. 7
2.3 The Ramberg-Osgood curve from EC9. f_O is the proof strength defined by the 0.2% offset method. f_x is the stress level at ϵ_{max} strain. $\epsilon_{O,x}$ is used to define the Ramberg-Osgood exponent n_{RO}. 10

3.1 Schematic figure from *CG-0128 - Buckling* of design curves as function of slenderness. σ_{cr} and σ_{eH} denotes the critical stress and specified minimum yield stress, respectively. λ is the slenderness parameter. 12
3.2 Non-uniform stress distributions along the edges of the plate due to deflections induced by buckling and/or lateral loads [15]. 14
3.3 The different failure modes of stiffened panels subjected to combined axial loading from Paik and Kim's benchmark study. a) Overall collapse b) Biaxial compressive collapse c) Beam-column type collapse d) Local buckling of stiffener web e) Flexural-torsional buckling / Tripping. [20] 16
3.4 Buckling of a longitudinally compresses panel. a) Overall Buckling b) Torsional Buckling c) Plate Buckling. 17
3.5 The different models used to analyse buckling of stiffened panels [10]. 18

4.1 Illustration of the partial factor method . Note that the characteristic values always are chosen unfavorably and partial safety factor is larger if the uncertainty is more severe[1]. 20

5.1 Illustration of Snap-Through and Snap-Back for static analysis[24] 42

6.1 The stiffened aluminium panel modelled with Abaqus. 43
6.2 Stress-Strain relations of the chosen aluminium alloys. Each true stress-strain point represents a data point used in Abaqus, but with plastic strain. 51
6.3 The HAZ pattern of the plate. 52
6.4 The HAZ pattern of the plate and the stiffener web. 52

6.5 The stiffener mesh. There are 5 elements along the height(76 mm) of the stiffener. The flanges have one element on each side of the web. The density in the x-direction is similar to the plate mesh. . . . 53
6.6 The plate mesh. The red line indicates the plate-girder connection. Note that there are two rows of 15 mm x 15 mm elements in the HAZ below the red line and between the girders. The other elements out side of the girders are 15 mm x 30 mm. 53
6.7 The girder mesh was created to fit perfectly with the plate and web mesh, such that the nodes would coincide. The stiffener comes into the frame from the left. 54
6.8 The transverse girder mesh. The red line shows the intersection with the plate and web. 54
6.9 The deformation of mode 1 from eigenvalue buckling analysis. The deformations are scaled up 100 times. 55

7.1 The Uy and Uz movement of the node that had largest lateral deformation for P6-WF8-T8. Note how the change in Uz coincides with ULS. . . 57
7.2 Panels with different dimensions. The applied axial load pressure during Riks analysis and associated axial deformations of the straight load edge. 60
7.3 Panels with different HAZ patterns. The applied axial load pressure during Riks analysis and associated axial deformations of the straight load edge. 60
7.4 Panel P6-SF8-T10 at the point of maximum capacity. Top: Mises stress. Bottom: Axial deformation. 61
7.5 Panel P6-SF8-T10 at the point of maximum capacity. Top: Transverse deformation (y-direction). Bottom: Lateral deformation (z-direction). The black star marks the node that had largest lateral deformation. 62
7.6 The combined cross-sectional area of the stiffener and plate correlates linearly with the axial ULS pressure load. 63

8.1 The P6-WF8-T10 at maximum resistance capacity. Deformations are scaled 30x. 69

Tables

4.1 The obtained alloy properties from EC9. f_0 is the 0.2% proof strength and f_u is thee ultimate tensile strength. 22
4.2 The extent of HAZ according to EC9. 24
4.3 Allowable bending stresses in plates and stiffeners[N/mm^2] 32
4.4 Definitions of coefficients B and e_0 35

6.1 Dimensions of the panel. The subscripts p, w, f, g denotes values for the plate, web, flange and girder, respectively. The underlined values are the values of the base panel model, while the other are dimensions of alternative panels that were also analysed. 45
6.2 The obtained alloy properties from EC9. f_0 is the 0.2% proof strength and f_u is thee ultimate tensile strength. 46
6.3 The boundary conditions of the panel. **Edge set 1:** Plate, web and flange edges at the fixed short end. **Edge set 2:** Plate, web and flange edge at loaded short side. **Edge set 3:** Plate edges of both long sides (not girder edges). **Edge set 5:** Top edges of transverse girders. 48

7.1 Results from Abaqua Riks-analysis of the ultimate strength of stiffened aluminium panels in uniform axial compression. σ_{ULS} denotes the maximum achieved load pressure and U_x denotes the axial deformation of the plate edge at that point. $\%\Delta\sigma_{ULS}$ denotes the percentage change of σ_{ULS} relative to the base case P6-SF8-T10 and $\%\Delta A$ denoted the percentage change of the cross sectional area relative to the base case (only stiffener and plate). ΔA refers to the area that have been changed. The name Px-SFy-Tz refers to a panel with dimensions t_P=x mm, t_W=t_F=y mm and t_T=z mm. 58
7.2 Design resistance of panel with length 950 mm and 3 T-stiffeners according to EC9. Dimensions are similar as to in Chapter 6, but with only the panel part in between the girders. 64
7.3 Design Resistance of plate with dimensions 232 mm x 950 mm. The dimensions are smaller than the regular panel because the thicknesses t_w = 8mm and t_g =10 mm are subtracted. 64

7.4 Design resistance of panel with length 950 mm and 3 T-stiffeners according to EC9. Stiffened panel analysed with Abaqus. Reduction of EC9 relative to Abaqus result. 65
7.5 Design resistance of panel with length 950 mm and 3 T-stiffeners according to EC9. Note that 2) stresses are lower because the web is considered slender and is reduced due to local buckling. 65

Nomenclature

Abbreviation

ALS	Accidental Limit State
BC	Material Buckling Class
CSC	Cross-Section Class
EC0	Eurocode - EN 1990
EC1	Eurocode 1 - EN 1991
EC9	Eurocode 9 - EN 1999
FEA	Finite Element Analysis
FEM	Finite Element Method
FLS	Fatigue Limit State
FSW	Friction Stir Welding
HAZ	Heat Affected Zone
HSLC	High Speed and Light Craft
LRFD	Load and Resistance Factor Design
LSD	Limit State Design
MIG	Metal Inert Gas
NFEA	Nonlinear Finite Element Analysis
R_{xx}	Rotation about axis parallel to the x-axis
R_{yy}	Rotation about axis parallel to the y-axis
R_{zz}	Rotation about axis parallel to the z-axis
Riks	Riks modified method

SLS Service Limit State

TIG Tungsten Inert Gas

ULS Ultimate Limit State

wt% Weight percent

Greek Letters

β_9 Eurocode 9 slenderness parameter

χ Reduction factor for weld softening

Δ Vessel displacement

ϵ Strain

ϵ_9 Eurocode 9 parameter

ϵ_{Eng} Engineering strain

ϵ_{True} True strain

γ_{M1} Partial Safety factor for member

κ Reduction factor dependent on the buckling mode

λ Slenderness

ν Poisson's ratio

ω_i Vector of eigenvalues, Abaqus Theory

$\overline{\lambda}$ Reduced slenderness

Ψ Ratio of the smaller and larger applied stress

ρ Density

ρ_c Thickness reduction factor

$\rho_{O,haz}$ Proof strength reduction factor due to HAZ

$\rho_{u,haz}$ Ultimate strength reduction factor due to HAZ

σ Stress

σ_E Elastic buckling stress

σ_x Total normal stress in x-direction

σ_Y Tensile yield strength

σ_y	Total normal stress in y-direction
σ_{Eng}	Engineering stress
σ_O	0.2% proof strength
σ_{sl}	Stress induced from slamming load
σ_{True}	True stress
σ_{xy}	Total shear stress
τ	Shear stress
I_y	Second moment of area about y-axis

Latin Letters

a	Girder spacing or long length of plate
b	Stiffener spacing or short length of plate
b_f	Width of flange
b_{haz}	Extent of heat affected zone
D	Plate stiffness
E	Young's modulus of elasticity
f_1	
G	Shear modulus
h_g	Height of transverse girder
L_a	Total length in x-direction
L_b	Total length in y-direction
R_{eH_p}	Specified minimum yield strength of plate
t	Thickness
w	Lateral displacement
Z	Section modulus

Subscripts

9	Eurocode 9 parameters
c	Critical
E	Ideal Elastic Stress
Ed	Design load
eff	Effective value
f	Flange
g	Transverse girder
haz	Heat affected zone
i	i-th element or placeholder for arbitrary letter
o	0.2% offset value or proof strength
p	Plate
Rd	Design resistance
RO	Ramberg-Osgood
Sl	Slamming
stiff	Stiffener
u	Ultimate tensile strength
ULS	Ultimate strength
w	Web

Chapter 1

Introduction

1.1 Scope

Buckling of stiffened aluminium panels
Knekking av avstivede aluminiumspanel

Stiffened panels in aluminum are frequently used ship building, e.g. in high speed vessels, work boats for fish farming activities, service vessels for wind farms etc. They may also be used in deck girders for bridges. The stiffeners may be conventional T-, L- or Bulb-profiles or hat profiles. The transition in girder webs is normally configured with cutouts, potentially with secondary stiffening. To save fabrication costs the stiffeners are sometimes attached to the plate with staggered welding. Another option that has been utilized to ease fabrication is the so-called "floating frames" concept, where prefabricated panel sheets are "wrapped" around the transverse frames.

Recently a PhD-project on robotic welding of aluminium ship panels based on TIG and MIG welding has been started. It includes development of specialized ship designs that are optimized for robotic welding. An important part of the project is to ensure that the new design solutions satisfy existing design rules for ship hulls and to propose modified requirements when this is necessary. The work will among others comprise:

- Overview of present local and global design rules and design requirements as regards serviceability (SLS) fatigue (FLS), ultimate strength (ULS) and resistance to accidental actions (ALS) for aluminium ship structures
- Identification of possible structural configuration of stiffened panels, stiffener/frame connection etc. which are favourable wrt. robotic welding
- Modelling of structural for structural analysis of structural connections, structural components and entire hull for SLS, FLS, ULS and ALS analysis s by means of finite element software (e.g. LS-DYNA, ABAQUS, SESAM).

- Fluid/ice-structure interaction may be included where relevant, e.g. in the analysis of slamming
- Propose new rule formulations for design verification.

The objective of this work is to contribute to this project by investigating the buckling strength of stiffened panels.

The work is proposed carried out in the following steps:

- A brief description of the structural configuration of stiffened panels in the hull of high-speed vessels, ferries etc. built in aluminium with emphasis on conventional frames
- A review of relevant design criteria for stiffener, plates, frames and hull girders for High Speed Light Crafts (HSLC) according to DNV GL. Review of Eurocode 9 requirements for aluminium structures.
- Describe the material properties of relevant aluminum alloys for shell plating and stiffeners Discuss how the material properties, residual stresses and initial imperfections are affected by welding. Describe how these effects can be modelled in nonlinear finite element analysis
- Perform parametric analysis of stiffened panel by means of nonlinear finite element analysis with Abaqus. The geometries of the panel to be selected in agreement with the supervisor. A detailed description of modelling strategies shall be included, notably w.r.t panel length and boundary conditions.
- Conduct linear eigenvalue analysis of the panels and compare finite element results with simple design formulas. Introduce imperfections and conduct nonlinear ultimate strength analyses of the panels with different stiffener geometries and plate thicknesses. Compare results with design formulations. On the basis of the results improved design formulations may be proposed
- Conduct linear eigenvalue analysis of the panels and compare finite element results with simple design formulas. Introduce imperfections and conduct nonlinear ultimate strength analyses of the panels with different stiffener geometries and plate thicknesses. Compare results with design formulations. On the basis of the results improved design formulations may be proposed
- Conclusions and recommendations for further work

Literature studies of specific topics relevant to the thesis work may be included.

The work scope may prove to be larger than initially anticipated. Subject to approval from the supervisors, topics may be deleted from the list above or reduced in extent.

In the thesis the candidate shall present his personal contribution to the resolution of problems within the scope of the thesis work.

Theories and conclusions should be based on mathematical derivations and/or

logic reasoning identifying the various steps in the deduction.

The candidate should utilise the existing possibilities for obtaining relevant literature.

Thesis format The thesis should be organised in a rational manner to give a clear exposition of results, assessments, and conclusions. The text should be brief and to the point, with a clear language. Telegraphic language should be avoided.

The thesis shall contain the following elements: A text defining the scope, preface, list of contents, summary, main body of thesis, conclusions with recommendations for further work, list of symbols and acronyms, references and (optional) appendices. All figures, tables and equations shall be numerated.

The supervisors may require that the candidate, in an early stage of the work, presents a written plan for the completion of the work. The plan should include a budget for the use of computer and laboratory resources which will be charged to the department. Overruns shall be reported to the supervisors.

The original contribution of the candidate and material taken from other sources shall be clearly defined. Work from other sources shall be properly referenced using an acknowledged referencing system.

Thesis supervisor

Prof. Jørgen Amdahl

Chapter 2

Aluminium as Structural Material

2.1 Introduction of Aluminium Properties

Aluminium is a material used extensively for marine applications due to the high specific strength exhibited in most aluminium alloys. The density of aluminium is $\sim$2700 kg/m^3, which is approximately $1/3$ that of steel at $\sim$7850 kg/m^3. Aluminium has a modulus of elasticity of about 70 000 MPa, which again is about $1/3$ that of steel at 200 000 MPa. Thus the buckling resistance of an aluminium cross-section is lower than an equal cross-section of steel. Another consequence is that deflection checks are more often the critical design checks in aluminium structures. Aluminium's strength-to-elastic ratio is about twice that of standard steels[1]. Aluminium has a Poisson's ratio of about 0.33 and a shear modulus of $\sim$ 26 000 MPa.

An appreciated benefit to aluminium compared to steel is its lack of a temperature transition. This lack results in aluminium becoming much less brittle than steel. For some applications, this low-temperature ductility is very useful. Furthermore, some of the 5xxx alloys are so corrosion-resistant, that it is possible to save money on maintenance, as even painting becomes optional [2].

However, some challenges arise with the use of aluminium, such as galvanic corrosion, general corrosion in the marine environment, corrosion fatigue, low melting point (660 °C), loss of strength above only 95 °C, lower fracture toughness than steel and more prone to buckling and large deflections. Aluminium is also more expensive, but for some vessel types, the lighter, faster and more fuel-efficient hull of an aluminium vessel justifies the added cost[3].

2.2 Aluminium Alloys and Tempers

Alloy Series

Aluminium comes in a great variety of different series, based on the added alloy elements. Aluminium alloys are classified in a global series system, ranging from 1xxx to 8xxx depending on the alloying elements. In modern shipbuilding, the 5xxx series and 6xxx series are almost the only alloy series used [4], and they are the only series accepted by DNV GL's classification rules *RU-SHIP* and *RU-HSLC*. The other alloys are not considered corrosion-resistant enough.

Temper

The two main temper methods to improve the strength of aluminium alloys are heat treatment and strain hardening, denoted *T* and *H*, respectively. Other tempers are *F* for *as fabricated*, *O* for *annealed* and *W* for *solution heat-treated*. Be advised that the same alloy and temper might have different material properties in different products. For example, the 6060-T6 sheet has a minimum tensile ultimate strength of 290MPa, while the 6060-T6 extrusion has a minimum tensile ultimate strength of 260MPa [5].

2.3 The 5xxx Alloy Series

The 5xxx series has magnesium as the primary alloying agent and is among the more widely used aluminium alloys. The added magnesium greatly increases the strength with only a minor reduction to ductility. For current wrought alloys, the magnesium content does not exceed 5.5 wt% [6]. The series generally has good weldability properties, high resistance to corrosion, moderate to high strength characteristics and may be strengthened by cold working [5]. 5xxx alloys can, however, not be heat-treated. The 5xxx series is often found on sheets and rolls and is used for deck and hull plating[4]. AA5083 is widely used in marine aluminium applications, as well as AA5383 and AA5059. The AA5383 alloy is often considered the improved AA5083. AA5083 and AA5383 should normally be in the H116 or H321 temper according to DNV GL's *RU-SHIP*[7]. Both are fabricated to have corrosion resistance.

Strain-Stress Properties of the 5xxx alloys

The 5xxx alloys generally have very rounded stress-strain curves compared to steel and the 6xxx alloys. The local tangent modulus of the 5xxx series may fall significantly below the elastic modulus before proof stress is reached[4]. Another aspect of the 5xxx series that is often overlooked is that because it is strain hardened, the proof stress is often higher in tension than compression [4].

2.4 The 6xxx Alloy Series

The 6xxxx series has magnesium and silicon as its primary alloying elements and have up to 1.5 wt% silicon. Silicon is added for precipitation of Mg_2Si, and it should have this ratio or excess of silicon. The 6xxx series may be heat-treated and cold worked[8]. The hardening induced by precipitation of Mg_2Si reduces ductility because of segregation of silicon in the grain boundary region. The 6xxx series inhibit fair localised seawater corrosion resistance, but not as good as the 5xxx series [6]. The 6xxx alloy series is, along with 1xxxx and 3xxxx series, considered *soft* because it is more easily and economically extruded than other aluminium alloys [5]. It is commonly found as extruded profiles and used as structural reinforcements, bulkheads and stiffeners [4]. The 6xxx series should typically not be in contact with seawater, and it is specified by DNV GL *RU-HSLC* that it is only allowed under special consideration.
The AA6082 alloy (with T5 and T6 temper), which was first registered in 1972, has become very popular in European shipbuilding [5]. Its allowable tensile strength, which is dependent on thickness, is 10-18% higher than the very popular, general-purpose AA6061, and it generally has better corrosion resistance due to lower copper content. Their extrudability and anodising response are about equal[5]. The T6-temper means that the material was solution heat-treated and artificially aged.

Strain-Stress Properties of the 6xxx alloys

The stress-strain curve of the 6xxx alloys are in general less round and more similar to the elastic perfectly-plastic assumption often used in the analysis of steel structures [4]. An issue ,however, is that these alloys might show quite anisotropic behaviour after extrusion. The 6xxx alloys are typically less ductile and have lower strength in stress directions vertical to the extrusion direction [4].

2.5 Residual Stresses and Distortions

Residual stresses are stresses present in a material, even with an absence of external loading.[9] They may be purposefully induced for some products, such as in tempered glass, but are often undesirable effects from fabrication and welding processes. Steel and aluminium, like most solids, expand when it gets heated and contract when it cools. When structural members are fabricated there is an uneven temperature gradient within the member, because the areas close to the surface cools faster than the inner volume[10]. For a butt weld in a plate, tension stress develops close to weld and are balanced by compressive forces further out in the plate [9]. In buckling theory of plates, it is common to assume that the maximum compressive stresses, thus first yield, occurs at the plate's edge. However, because of tensile residual stresses induced by the welding process, the first yield typically occurs slightly further into the plate [9]. The ship hull is dynamically loaded, and therefore the residual stresses will gradually decrease. Therefore, it is uncertain

if best practice includes partially including or excluding the residual stresses [9]. As a consequence of the low elastic modulus and low melting point, the distortions in aluminium members are typically larger than those in steel members[11]. This is reflected in the classification, where the distortion tolerances for aluminium are less strict than those of steel. It is difficult to predict the steel distortions induced by fabrication and welding, but even more difficult for aluminium, as even less data is available.

Residual Stresses in Panels

Kristensen [12] analysed the effects of residual stresses for simply supported rectangular 6082-T6 plates using Abaqus. The plates had heat-affected zones around the edges due to welding, which also included tensile residual stresses. The tensile residual stresses were chosen to be 45% of σ_o. The residual stresses resulted in a 2%-5% reduction of axial strength capacity. Zha and Moan(2001 [13], 2003 [14]) studied the effects of residual stresses in flat bar stiffened 6082-T6 panel and found that it reduced the ultimate strength by about 3%.

Residual stresses in Sections

The effects of residual stresses in rolled sections are mainly dependent on geometry and uneven cooling. The flange tip, for instance, cool faster than the flange root, thus creating tensile and compressive residual stresses in the root and tip, respectively. The residual stresses are typically more severe in sections with wide flanges[10].

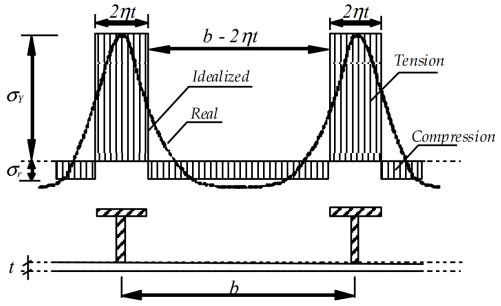

Figure 2.1: Residual stresses induced by welding [15].

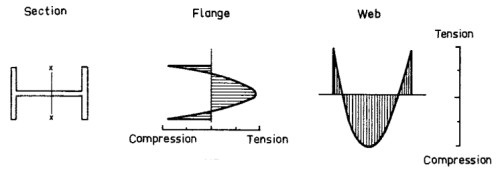

Figure 2.2: Residual stresses induced by rolling [10].

2.6 Heat affected Zone

Welding effects and welding quality are among the most difficult aspects of building aluminium structures compared to steel. There are almost always significant strength reductions in the heat-affected zone. This reduction is an important difference compared to steel, in which the HAZ has little to no effect on elastic buckling strength[4]. The HAZ size from fusion welding is typically about 3 times the e plate's thickness from the weld centre line [4], but this varies with welding parameters. Also, aluminium is very reactive, and the welds are susceptible to porosity, cracked shrinkage and large HAZ extent[16]. Because aluminium melts at a much lower temperature and its stiffness is about one-third of steel, there tend to be larger distortions induced by aluminium welding and fabrication compared to steel [11].

HAZ strength Reductions

The most significant strength increases from alloying elements like copper, magnesium and silicon come from heat-precipitation and cold working. In other words, those that have T5-T10 and/or H1-H4 tempers. Welding reduces the strength because heating tends to reduce or even erase the temper strength increases. Arc welding, i.e., melts a localised region, which leads to significant strength decreases of the structure in the HAZ. The 5xxx series is only cold-worked, so its strength is reduced back to its annealing strength[4]. The 6xxxx series has been cold-worked and heat-treated. Thus its strength is reduced to slightly below the solution-heat-treated strength, which is the T4 temper. The strength reductions must be accounted for when the buckling strength is assessed. The tendency is that the high strength alloys with large quantities of copper like the 2xxx and 7xxx alloys have large strength reductions and can be hard to even weld at all. The 5xxx series are generally among the alloys with strongest HAZ properties; i.e. the 5086-H112 plate with 12.5mm thickness only reduces its strength from 250MPa to 240MPa. Keep in mind that the HAZ's effect on fatigue strength needs to be accounted for with both steel and aluminium.

2.7 Welding Methods

Even though the principles are the same, the welding parameters and techniques differ sufficiently that welders typically specialise in one material type. The most common welding technique is gas-metal arc welding (MIG). The only option used to be gas-tungsten arc welding (TIG), which is used for thinner samples. Another method from the 90' that has been improved and gained popularity during the last decades is friction stir welding [11]. One benefit of friction stir welding is that it may induce significantly lower temperature in the material than MIG. Thus it may be possible to reduce the peak tensile stress[17] and extent of HAZ.

Weld Quality

The weld quality is dependent on the following parameters [16]:

- Welding process(MIG/TIG/FSW)
- Thickness of the welded part
- Welding speed
- Preheating
- Filler alloy

2.8 Ramberg-Osgood

The stress-strain properties of aluminium alloys are often listed with parameters to be used with the Ramberg-Osgood formulation[18]. It does not always accurately predict the whole stress-strain curve, but it has the advantage of being simple and useful to implement[4]. With the Ramberg-Osgood formulation, the strain may be formulated as follows:

$$\epsilon(\sigma) = \frac{\sigma}{E} + 0.002\left(\frac{\sigma}{\sigma_0}\right)^{n_{RO}} \tag{2.1}$$

where:
σ_0 [MPa] is the proof stress with a 0.2% strain offset,
E [MPa] is Young's modulus of elasticity,
n_{RO} [-] is the Ramberg-Osgood exponent (also called the knee factor).

The Ramberg-Osgood formulation is typically listed with its parameters in classification rules, but may also be computed based on material test data. A common strategy is to calculate it based on the 0.2% proof strain and some x% strain. Two lines with the same slope as Young's modulus are drawn. The first starting at 0.2% strain and the second at x% strain, such that x%>0.2%. The proof stress, σ_x, is taken as the intersection with the first line and σ_x is taken as the second intersection, such that σ_x is close to the highest stress values to be used in ensuing analyses. The formula to estimate the Ramberg-Osgood exponent is

$$n_{RO} = \frac{\ln(0.002/\epsilon_{O,x})}{\sigma_0/\sigma_x} \tag{2.2}$$

The offset method

Many aluminium alloys, including the 5xxx and 6xxx series, exhibit nonlinear stress-strain behaviour at stress levels significantly lower than yield. The 0.2% offset method is a common approach to determine the proof strength of aluminium alloys. In the 0.2% offset method, the proof strength is determined to be the point where the stress-strain curve of a specimen test crosses a linear curve with a slope equal to E and an offset of 0.2% strain [4]. The proof strength with a 0.2% offset

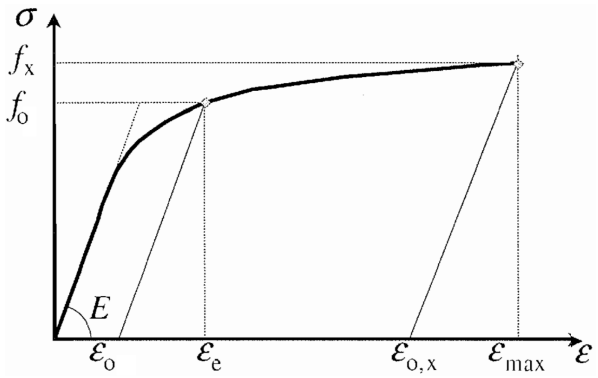

Figure 2.3: The Ramberg-Osgood curve from EC9. f_O is the proof strength defined by the 0.2% offset method. f_x is the stress level at ϵ_{max} strain. $\epsilon_{O,x}$ is used to define the Ramberg-Osgood exponent n_{RO}.

is commonly agreed to represent the yield strength. It is used in *Eurocode 9* and DNV GL's *RU-SHIP/RU-HSLC*.

Chapter 3

Panel Buckling Theory

3.1 Buckling Intro

Buckling is a structural phenomenon that may occur in slender structures. It is characterised by a sudden deformation change perpendicular to the loading direction as a consequence of increased loading. Buckling is most commonly associated with compressive loading, but shear loads and in-plane moments may also induce buckling of plates. In theory, buckling of straight, slender structures are bifurcation problems, because no lateral deflection will occur until the critical buckling stress σ_E is reached, at which point it is unstable and snaps into a buckling deflection, of which direction it may be impossible to predict. In reality, however, structures will always have slight initial distortions that initially increase slightly with increased loading[9]. The rate of deflection increases with higher loading, and eventually, the resistance of the member decreases. Sometimes, the initial buckling deformation induced by the loading is unstable, and the panel may snap to a more stable buckling shape [9]. Whether or not the onset of buckling is a critical limit state depends on the structural type and its stability in the post-buckling range. A plate which is properly supported along the edges is stable in the post-buckling range, meaning that it increases its resistance with increased deflection until it collapses due to excessive yielding. Columns, however, are unstable, and their resistance decreases in the post-buckling range.

The study of panels and plates consists of several models and formulas describing some idealized condition. The model may describe the critical loads of pure torsional, pure shear, pure lateral or pure axial compressive forces. The common approach for design purposes is to solve idealized critical loads independently, then use some interaction formula to describe the critical combined load[15].

3.2 The slenderness Parameter

The slenderness parameter is used to classify structures based on how prone they are to buckling. In DNV GL's *CG-0128 - Buckling* the slenderness parameter λ and the classification of slenderness are defined as follows:

$$\lambda = \sqrt{\frac{Yield}{Elasticbuckling}} \tag{3.1}$$

where:

Slender structures	$\lambda > 1.4$	(3.2)
Moderate slender structures	$0.6 < \lambda < 1.4$	(3.3)
Stocky Structures	$0.6 > \lambda$	(3.4)

The compressive failure mode of moderate slender structures can not be fully described by pure elastic buckling formulas or pure yield assessments. Therefore some interaction formula is needed to bridge the gap between the two failure modes. Some of the popular interaction formulas, such as Johnson-Ostenfeld and Rankine, are shown in a figure in DNV GL's *CG-0128 - Buckling*, see Section 3.2. Note that using elastic buckling formulas or yield-based formulas outside of their respective domain give non-conservative results. Also note that slender, properly supported plates have an ultimate capacity higher than the elastic buckling stress.

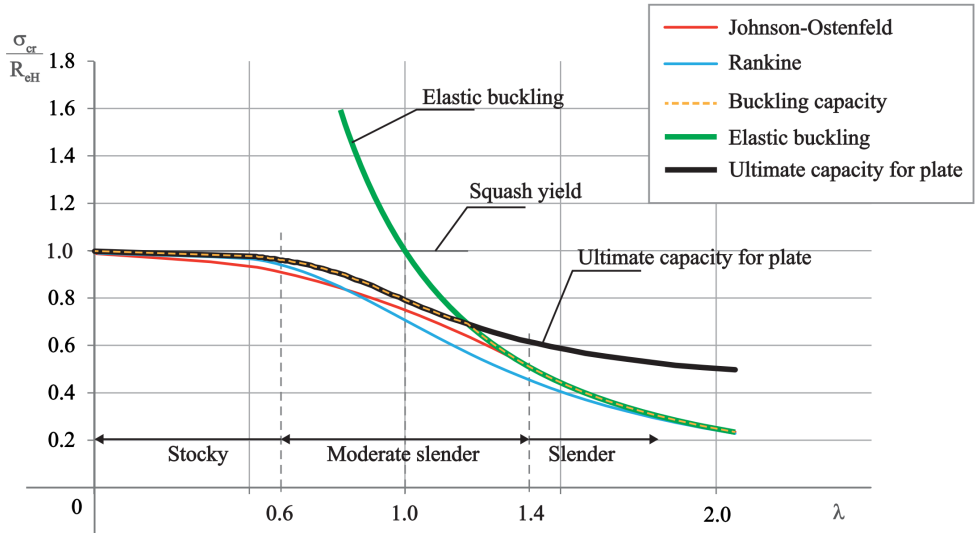

Figure 3.1: Schematic figure from *CG-0128 - Buckling* of design curves as function of slenderness. σ_{cr} and σ_{eH} denotes the critical stress and specified minimum yield stress, respectively. λ is the slenderness parameter.

3.3 Buckling of Initially Perfect Plates

In *Theory of elastic stability* [19], Timoshenko investigates the equilibrium equation of an initially perfect thin plate that is deflects slightly by the action of a small lateral load, q. The equilibrium can be expressed as:

$$\nabla^4 w = \frac{\partial^4 w}{\partial x^4} + \frac{\partial^4 w}{\partial x^2 \partial y^2} + \frac{\partial^4 w}{\partial y^4} = \frac{1}{D}\left(q + \sigma_x\, t \frac{\partial^2 w}{\partial x^2} + 2\sigma_{xy}\, t \frac{\partial^2 w}{\partial x \partial y} + \sigma_y\, t \frac{\partial^2 w}{\partial y^2}\right), \tag{3.5}$$

where the plate stiffness,D, is defined as $D = \frac{Et^3}{12(1-\nu^2)}$ and w is the lateral deflection.

For a simply supported rectangular plate that is uniformly compressed in one direction and has no lateral load, $q = 0$, the deflection shape is described by:

$$w(x,y) = \sum_m \sum_n C_{mn} \sin\frac{m\pi x}{a} \sin\frac{n\pi x}{b}, \tag{3.6}$$

where m and n are the number of half waves in x- and y-direction[19]. The variables a and b denotes the length and width of the plate, respectively.
The magnitude of the compressive force per unit length equals σ_x t and is slowly increased. The initially perfectly flat plate will eventually reach the unstable bifurcation point and buckling will occur. The critical value can be found by integration of the equilibrium equation or by considering the conservation of energy in the system. The critical compressive load is

$$N_E = \frac{\pi^2 D}{a^2}\left(m + \frac{a^2}{mb^2}\right)^2, \tag{3.7}$$

which corresponds to only one half-wave in the perpendicular direction, but there can be several half-waves in the direction of the compression, which depends on the length of the plate.
From Equation (3.7) it is possible to derive the elastic buckling stress, which is expressed in Equation (3.8), where $k(\geq 4)$ is a buckling factor dependent on the number of buckling half waves, which again is dependent on the aspect ratio a/b. The minimum critical stress of a uniformly compressive loaded plate occurs when the length is a multiple of the width. The elastic buckling stress is

$$\sigma_E = \frac{\pi^2 E}{12(1-\nu^2)}\left(\frac{t}{b}\right)^2 k \tag{3.8}$$

Computing σ_E is relatively easy, but it is not a good estimate of the ultimate strength. It may give a good indication of which failure modes are more likely and provide a foundation for more complex inelastic analysis[10].

3.4 The Effective Thickness Method

As stated in the introduction of this chapter, given sufficient edge constraint, slender plates may carry loads substantially in excess of the elastic prediction. In the effective thickness method, edges are typically constrained to be simply supported and forced to remain straight. The lateral deflections from buckling induce member stresses in the transverse direction and non-uniform stresses along the unloaded edge. The effective thickness of simply supported plates with unloaded edges forced to remain straight may be estimated by the following formula[15].

$$\frac{b_{eff}}{b} = \frac{\sigma_b}{\sigma} = \begin{cases} \frac{2}{\beta} - \frac{1}{\beta^2}, \text{ if } \beta \geq 1 \\ 1, \text{ if } \beta < 1 \end{cases} \tag{3.9}$$

where $\beta = b/t\sqrt{\sigma_Y/E}$. When the effective thickness theory is used, the ultimate capacity of the panel is assumed to coincide with the onset of yielding at the unloaded edge. The variation in stresses along the edges, due to finite lateral deflections are illustrated in Section 3.4.

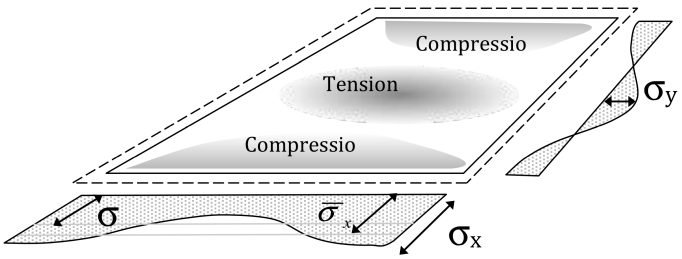

Figure 3.2: Non-uniform stress distributions along the edges of the plate due to deflections induced by buckling and/or lateral loads [15].

Ship Panel Ultimate Failure Mode [10]

In a benchmark study from 2001 by Paik and Kim [20] the failure of stiffened panels subjected to combined axial load, in-plane bending and lateral pressure where examined. The modes were categorized into six collapse modes, which are illustrated in Section 3.4 and described as follows [10]:

- Mode I: Overall collapse of the plating and stiffeners as a unit, see Fig. Section 3.4(a),
- Mode II: Biaxial compressive collapse without failure of the stiffeners , see Section 3.4(b),
- Mode III: Beam-column type collapse , see Fig. Section 3.4(c),
- Mode IV: Local buckling of the stiffener web (after the inception of the buckling collapse of the plating between the stiffeners), see Section 3.4(d),
- Mode V: Flexural–torsional buckling or tripping of the stiffeners, see Section 3.4 e),
- Mode IV: Gross yielding

The likelihood of each failure mode is dependent on the relative stiffnesses of the plate and stiffeners, as well as the loading conditions. Collapse mode I may happen if the stiffeners are relatively weak, but the stiffeners of ships are usually required to be at least as strong as the plating to avoid overall buckling.

Mode II may occur as a result of predominantly bi-axial compressive loads. The collapse starts as yielding of the plate at the stiffener-plate intersection at the edges. For collapse mode II, the ultimate strength of the panel may be simplified as the ultimate strength of the most highly stressed plating between the stiffeners.

When the relative stiffener strength is intermediate, the stiffened panel is likely to collapse like a beam-column, like in collapse mode III. With a high height to thickness ratio of the stiffener, local plate buckling between the stiffeners may induce local buckling of the web, which refers to mode IV. Collapse mode V is often called tripping or flexural-torsional buckling. It occurs when the stiffener flanges are unable to remain straight, which causes the web and flange to twist sideways. For collapse mode III, IV, and V, the ultimate panel strength may be estimated as the ultimate strength of the most stressed stiffener.

Collapse Mode VI may occur in stocky (or predominantly tensile loaded) panels and is characterised by yielding of large parts of the cross-section without prior local or overall buckling. The checks for this collapse mode are based on the least favourable cross-section (i.e. smallest due to holes etc.) and is sometimes referred to as squashing strength.

The plate-stiffener panel is also supported by heavy longitudinal and transverse girders, but these are typically designed to be much stronger than the stiffener-plate panel. When the transverse girders, as well as the longitudinal stiffeners, buckle, its called overall grillage buckling, but this is very unlikely. Aluminium panels, however, tend to be more slender and lighter built than steel panels, and therefore the likelihood of coupled global and local buckling is increased [9].

3.5 Models for Buckling of Stiffened Plates

As for any structural analysis, the accuracy depends on the structural idealization model. The most relevant models for a stiffened steel or aluminium panel are described in the book *Ship Structural Analysis and Design* by Paik and Hughes [10] which forms the basis for this section. The models are shown in figure **??** and described below:

- a) plate-stiffener combination model;
- b) plate-stiffener separation model; and
- c) orthotropic plate model.

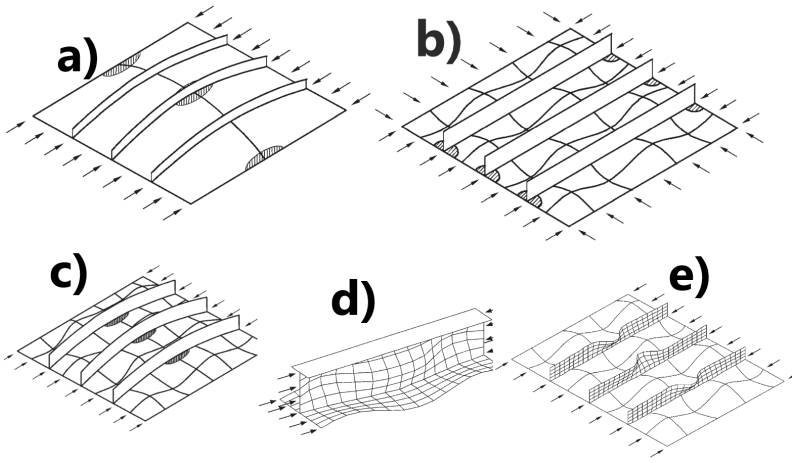

Figure 3.3: The different failure modes of stiffened panels subjected to combined axial loading from Paik and Kim's benchmark study. a) Overall collapse b) Biaxial compressive collapse c) Beam-column type collapse d) Local buckling of stiffener web e) Flexural-torsional buckling / Tripping. [20]

The combination model (also called beam-column model) narrows the analysis to a single beam with an associated plate. It is assumed that the flanges support bending moments while the stiffener webs resist shear loads. This model might be unreliable when the flexural rigidity of the stiffener is small compared to the plate stiffness, as torsional rigidity effects of transverse stiffeners and the Poisson ratio effect is neglected in this model.

In the separation model, the members are separated at the plate-web junctions. In this model, the plating in between the stiffeners is regarded as a plate in itself. This model is justified if local plate buckling and local buckling of the stiffener web are known to be the primary failure mode or are to be examined closer.

The orthotropic plate model may be used if the stiffeners are numerous, uniform, relatively weak and closely spaced in two orthogonal directions. In this model, the main rigidity of the system is in the plate, and the effects of the stiffeners are smeared into the plate with the effective width method.

The stiffener-plate structures in ship bottoms usually are longitudinally stiffened panels between larger transverse girders. The panel should typically be analysed with the combination model and the separation model. The heavy girder provides some rotational stiffness to the panel edges, but not infinite, and are typically modelled as simply supported. The heavy transverse frames might be analyzed by themselves, alas the separation model. In general, there is no one model that is superior on its own, but any individual model has its domain of utility, in example the separation model for denting and local buckling. The ultimate strength of a

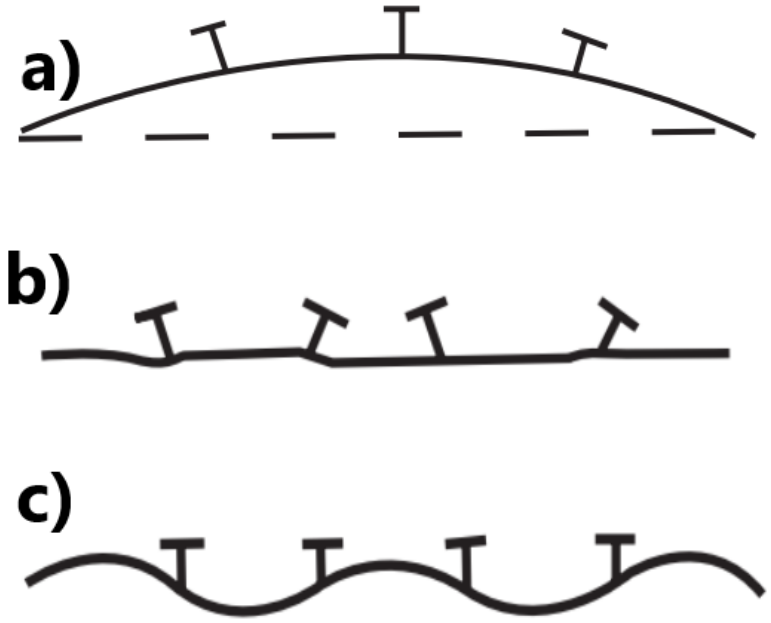

Figure 3.4: Buckling of a longitudinally compresses panel. a) Overall Buckling b) Torsional Buckling c) Plate Buckling.

panel is also typically determined based on the weakest mode of different buckling modes, and the different models may be used for different buckling modes.

3.6 The Effective Width Method

3.7 Residual Stresses

As described in Section 2.5 fabrication and welding of panels induce residual stresses that may reduce the panel ultimate strength. These residual stresses may, however, gradually be released. Due to low-cyclic loading of the hull girder, such as hogging and sagging, during ship operations in waves, the residual stresses are decreased especially quick. The effect of residual stresses in ship panels and the hull girder is often overlooked entirely or to some extent.

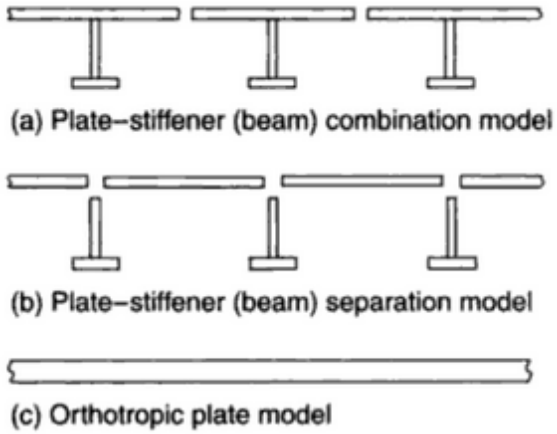

Figure 3.5: The different models used to analyse buckling of stiffened panels [10].

Chapter 4

Review of Eurocode 9 and HSLC

Technical standards are used to establish uniform engineering methods, processes, practices and technical criteria. In this chapter relevant design criteria for aluminium stiffener, plates, frames and hull girders in DNV GL's *High Speed Light Crafts (RU-HSLC)* will be reviewed. Relevant design criteria for aluminium structures according to *EC9* will also be reviewed. *RU-HSLC* applies specifically to high speed and light crafts, while Eurocode was established to be used in civil engineering. Both are based on the principles of Limit State Design. They are supposed to produce somewhat comparable results on the resistance of structures, but *RU-HSLC* does often not compute design resistances. In stead the main approach of *RU-HSLC* is to determine the minimum thickness or section modulus or some other parameter, as a function of the design load. The scope of this review will be limited to Ultimate Limit Strength assessment of buckling stability and material failure. Thus no structural integrity concerns regarding fatigue, accidents or corrosion will be assessed.

4.1 Background

4.1.1 Limit State Design

Both Eurocode and the DNV GL classification rules use the principles of Limit State Design (LSD), also called Load and Resistance Factor Design(LRFD). It is a structural assessment method in which the design criteria are checked against a set of limit states. There are always uncertainties when it comes to loads and resistances of structures. The ultimate capacity of identical panels, may for instance deviate due to slight differences in quality of welding, material or initial distortions. These uncertainties are taken into account by partial safety factors that scale up characteristic loads and scale down characteristic resistances, see Section 4.1.1. The scaling magnitude depends on the limit state and the severity of the uncertainty. The limit states defined by DNV GL in *OS-C101* are:

- **Service Limit State (SLS)**: Corresponding to the criteria applicable to normal use or durability

- **Ultimate Limit State (ULS)**: Corresponding to the maximum load carrying resistance
- **Fatigue Limit State (FLS)**: related to the possibility of failure due to the effect of cyclic loading
- **Accidental Limit State (ALS)**: Ensures that the structure resists accidental loads and maintain integrity and performance of the structure due to local damage or flooding.

Eurocode defines the limit states Service Limit State(SLS) and Ultimate Limit State(ULS) in EC0, with assessments such as E.g. fatigue, loss of static equilibrium or fire accidents as separate sets within ULS [**Eurocobook**].

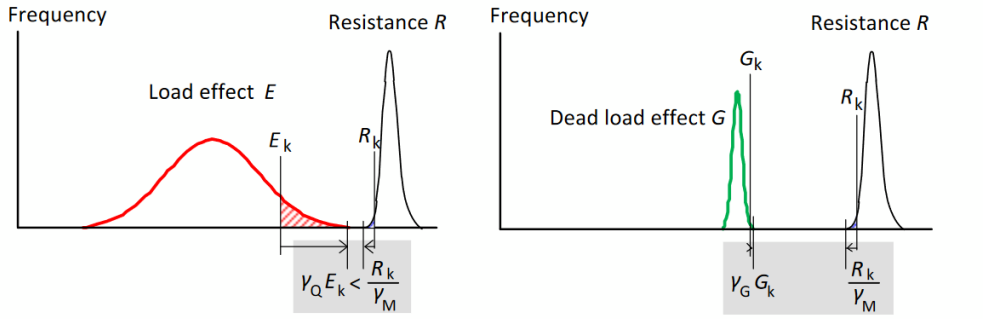

Figure 4.1: Illustration of the partial factor method . Note that the characteristic values always are chosen unfavorably and partial safety factor is larger if the uncertainty is more severe[1].

Where γ_Q, γ_G and γ_M are partial safety factors and E_k and R_k are the characteristic value of the load effects and the characteristic value of the resistance, respectively. They may relate to axial tension, compression, bending moment, shear or a combination, and may apply at a cross-section or on a connection. As illustrated in Section 4.1.1, the characteristic values are often conservative estimates such as 5%- and 95%-percentile.

Partial Safety Factors

Typical material safety factors are typically 1.1 (γ_{M1}) for members, 1.25 for connections that are welded (γ_{Mw}) and 1.25 for riveted or bolted (γ_{M2}) connections. In general the partial safety factor takes into account the uncertainty of different structural aspects. Therefore, relatively certain quantities such as self-weight have small safety factors.

4.2 Intro to Eurocode

The ten standards EN 1990 to EN 1999 were established by The European Committee for Standardization to harmonise the many national standards for buildings and civil engineering structures in Europe. They are often named *Eurocode0* (EN 1990) to *Eurocode9* (EN 1999)and will hereafter be Abbreviated *ECx*. *EC0* relates to the basis for structural design and specifies the partial safety factors on loads. Some of the factors might be overruled by the nationally determined parameters in the national annex of a country. *EC1* relates to design loads, none of which are relevant to ships. *EC3* to *EC9* refers to different structural building materials with aluminium structures in *EC9*.

4.3 Aluminium Properties in Eurocode 9

This section will mainly refer to *EC9*, but some references to *RU-HSLC* will occur. In *EC9* the modulus of elasticity, E, and Poisson's ratio, ν, shall be taken as 70 000 MPa and 0.3, respectively. *RU-HSLC* (and *RU-SHIP*) uses the same modulus of elasticity (unless stated otherwise), but a Poisson's ratio of 0.33. For strength assessments with *RU-HSLC*, the as-welded properties of the 5xxx series is in general to be taken in condition 0 or H111, while the 6xxx series must be taken in the most unfavourable temper, corresponding to T4.

The recommended minimum thickness of a aluminium material to be used with *EC9* is 0.6 mm and 1.5 mm for welded parts. This may be altered in the National Annex. The aluminium materials in *RU-SHIP/RU-HSLC* are valid in the range 3 mm to 50 mm. The main reason for this difference is the use cases of *EC9* and *RU-SHIP/RU-HSLC*.

4.3.1 Alloy Selection for Panel Buckling

EC9 and DNV GL does not list the aluminium alloys with the same tempers, and DNV GL does not provide parameters to determine the stress-strain curve, only ultimate tensile and compressive stresses. *EC9* was therefore used as reference for alloy data. 5083-H24 was chosen in plate condition for the plate of the panel and 6082-T6 was chosen for the stiffeners (extruded condition with the main loading in the same direction as the extrusion).

The yield criterion

The Von Mises yield criterion is used to assess critical points of the cross section and is formulated as follows.

In *EC9* f_o refers to the characteristic 0.2% proof strength for bending and overall yielding in tension and compression, while f_u refers to the ultimate tensile strength for the local capacity of a net section in tension and compression[1].

Table 4.1: The obtained alloy properties from EC9. f_0 is the 0.2% proof strength and f_u is thee ultimate tensile strength.

Alloy-Temper (EN-AW)	**Thickness** [mm]	f_o [MPa]	f_u [MPa]	$f_{o,HAZ}$ [MPa] 1)	$\rho_{o,HAZ}$	$f_{u,HAZ}$ [MPa] 1)	$\rho_{u,HAZ}$	**BC** 2)	n_{RO} 3)
5083-H24 4)	≤ 25	250	340	155	0.62	275	0.81	A	14
6082-T6 5)	$5< t\leq 15$	260	310	125	0.48	185	0.6	A	25
1) Valid for MIG welding and thickness up to 15 mm.									
2) Buckling Class 3) Ramberg-Osgood exponent									
4) Wrought sheet, strip, plate									
5) Wrought, Extruded profile									

4.4 Buckling Resistance of Members According to Eurocode 9

The buckling resistance of members are checked individually for axial compression, bending and both axial compression and bending. The buckling design resistance for axial compression, N_{ed}, shall be verified against both flexural and torsional-flexural and local squashing. Local squashing refers to gross yielding (of least favorable cross section), which typically is not the critical resistance for slender structures. The buckling resistance shall be taken as in Equation (4.1) unless structural-type specific formulations apply. Plates and stiffened panels, for example, have specific buckling resistance formulations.

$$N_{b,Rd} = \kappa \chi A_{eff} f_o / \gamma_{M1} \tag{4.1}$$

$$\chi = \frac{1}{\phi + \sqrt{\phi^2 - \overline{\lambda}^2}} \leq 1,0 \tag{4.2}$$

$$\phi = \frac{1}{2}(1 + \alpha(\overline{\lambda} - \overline{\lambda}_0) + \overline{\lambda}^2) \tag{4.3}$$

$$\overline{\lambda} = \sqrt{\frac{A_{eff} f_0}{N_{cr}}} \tag{4.4}$$

Where:
κ is a buckling mode dependent reduction factor,
χ is a reduction factor for weld softening,
A_{eff} is the effective area for class 4[1],
N_{cr} is the elastic buckling load,
α and $\overline{\lambda}_0$ are parameters dependent on the material buckling curve.
κ and χ are dependent on the relative slenderness $\overline{\lambda}$ and $\overline{\lambda_T}$ for flexural and torsional buckling, respectively. χ serves a similar purpose as the Jonson-Ostenfeld and Perry-Robertson transition curves, and is thus also influenced by the material buckling class (via α and $\overline{\lambda}_0$).

[1] $A_{eff} = A$ for cross-section class 1,2 and 3.

Yield

$$[h]\left(\frac{\sigma_{x,Ed}}{f_o/\gamma_{M1}}\right)^2+\left(\frac{\sigma_{z,Ed}}{f_o/\gamma_{M1}}\right)^2-\left(\frac{\sigma_{x,Ed}}{f_o/\gamma_{M1}}\right)\left(\frac{\sigma_{z,Ed}}{f_o/\gamma_{M1}}\right)+3\left(\frac{\tau_{Ed}}{f_o/\gamma_{M1}}\right)^2\leq C \quad (4.5)$$

$$\frac{\sigma_{x,Ed}}{f_o/\gamma_{M1}}\leq 1,\ \frac{\sigma_{z,Ed}}{f_o/\gamma_{M1}}\leq 1 \text{ and } \frac{\tau_{Ed}}{f_o/\gamma_{M1}}\leq 1 \quad (4.6)$$

where $\sigma_{x,Ed}$, $\sigma_{z,Ed}$ and τ_{Ed} are the design value of the local longitudinal stress, transverse stress and shear stress at the point of consideration. C ($\geq$1) is a constant that may be taken as 1.2 or may be determined in the National Annex.

4.4.1 Material Buckling Class

EC9 uses two material buckling classes, A and B, to account for differences in buckling resistance due to roundness of the stress-strain curves. Buckling class A is less prone to buckling. The materials with more rounded curves, i.e. lower Ramberg-osgood exponent, are in material buckling class B, while the materials with a sharper curve are in material buckling class A. The same alloy may have a different buckling class dependent on the temper.

4.4.2 HAZ softening adjacent to welds

In general, there is much emphasis on the welding process of aluminium, as it is much more delicate than welding steel. HAZ also have a significant effect on the buckling capacity of aluminium structures, while it is often considered negligible for steel structures. *EC9* assumes a constant level of strength reduction throughout the HAZ implemented as a reduced effective thickness. This assumption may not accurately describe HAZ behaviour, but its a easy to implement and conservative approach. In general, HAZ softening must be taken into account in the vicinity of any welds, unless the alloy is in the F or O condition and the strength is based on O condition properties. The reduction typically affects the 0.2% proof strength more severely than the ultimate tensile strength. There exists methods to mitigate the effects of HAZ softening after welding, however *EC9* does not provide any procedures to account for such improvements. The HAZ reduction factors are computed as

$$\rho_{c,HAZ}=\frac{f_{o,haz}}{f_o} \quad \text{, and} \quad (4.7)$$

$$\rho_{u,HAZ}=\frac{f_{u,haz}}{f_u}. \quad (4.8)$$

Due to natural ageing processes, the $f_{o,haz}$ and $f_{a,haz}$ values of the 6xxx series are only valid 3 days after welding. More time is needed if the temperature is below 10 °C.

The extent of HAZ for MIG welding is listed in Table 4.2. The width, b_{haz}, of the HAZ, is in general greater for TIG welding than MIG welding, because the heat input is higher.

Table 4.2: The extent of HAZ according to EC9.

Thickness	MIG	TIG
$0 < t \leq 6$ mm	20 mm	30 mm
$6 < t \leq 12$ mm	30 mm	
$12 < t \leq 25$ mm	35 mm	
$t > 25$mm	40 mm	

4.4.3 Cross-Section Class

EC 9 also have a four Cross-Section classes to be used for compressed parts, which are labeled 1 to 4 and defined as follows:

- Class 1 cross-sections are those that can form a plastic hinge with the rotation capacity required for plastic analysis without reduction of the resistance.
- Class 2 cross-sections are those that can develop their plastic moment resistance, but have limited rotation capacity because of local buckling.
- Class 3 cross-sections are those in which the calculated stress in the extreme compression fibre of the aluminium member can reach its proof strength, but local buckling is liable to prevent development of the full plastic moment resistance.
- Class 4 cross-sections are those in which local buckling will occur before the attainment of proof stress in one or more parts of the cross-section

The role of the cross-section class is to identify the extent to which the cross-section capacity is limited by buckling resistance. Class 4 is prone to local buckling and its compressive capacity must be reduced to take local buckling into account.

In general, the different parts of the cross-section may have different classes. The whole should be taken as the least favorable class in the member. The first step of determining the cross-section class of a compressed part is to determine the slenderness. The slenderness β is based on the width to thickness ratio, but also the stress gradient of the compressed part. Then the parameters β_1, β_2, β_3 are determined based on whether the part is an internal or outstand part, the material buckling class, whether the part has welds and the parameter $\epsilon = \sqrt{250/f_o}$. If $\beta > \beta_3$, the part is class 4.

4.4.4 Computing cross-section resistance

For determination of the cross-section resistance, *EC9* applies the effective thickness method reduce the capacity due to local buckling(class 4) and HAZ softening from

longitudinal welds. This is in contrast to *EC3* (for steel) in which the effective width method is used to build-up the effective cross-section. The effective thickness due to local plate buckling effects of class 4 compression members shall be taken as $t_{eff} = \rho_c t$. The effective thickness due to HAZ effects of longitudinal welds and local buckling within b_{haz} shall be taken as $t_{eff} = min(\rho_{o,haz} t, \rho_c t)$. ρ_c is computed based on the parameters β, ϵ, C_1 and C_2[2] and is computed as

$$\rho_c = \frac{C_1}{(\beta/\epsilon)} + \frac{C_2}{(\beta/\epsilon)^2} \quad \text{, if} \quad \beta > \beta_3 \tag{4.9}$$

Other strength reduction considerations

The HAZ softening effect of transverse welds is allowed for by the reduction factor $\omega_{x,haz}$ or $\omega_{xLT,haz}$. A cross-sectional part may be considered as without welds if the welds are transverse to the member axis and located at a position of lateral restraint. Shear lag effects are taken into account with the effective width method.

4.5 Estimation of Panel Buckling Resistance

In this section the buckling strength of a stiffened panel is estimated based on several *EC9* panel and plate formulations. This sections does not include all the details that went into the buckling resistance estimations. For all loading cases there are local squashing and yielding checks, but this will be ignored as the buckling checks are critical. In addition all partial safety factors, γ_{Mi}, can be disregarded as the aim is to compare with the Abaqus results.

The panel may be modeled as a multi stiffened panel, but for reasons of comparison several different models and formulation are computed.

Panel dimensions

The panel dimensions are similar to the P6-Sf8-T10 panel described and analysed in Chapter 6, but only the part in between the girders is analysed. That is, the panel has three longitudinal T-stiffeners with a height of 76mm, a flange width of 50 mm and a web and flange thickness of 8 mm. The stiffeners are situated b + b + b + b, where b equals 240 mm. The panel is 950 mm long (girder thickness is removed from length). The panel has heat affected zones on the plate on both sides of the web and on the web itself. The HAZ extent is 30 mm, see **??**. The aspect ratio is ≈1.

4.5.1 Stiffened Panel under Uniform Compression

κ is disregarded in the specific panel formulations of *EC9*, and here γ_{M1} is disregarded, so the new resistance stress is formulated as $N_{b,Rd} = \chi A_{eff} f_o$. The plating is

[2] C_1 and C_2 are also dependent on material buckling class and whether the part is with welds

regarded as an assemblage of identical column sub-units. χ for flexural buckling is computed for different panel types with N_{cr} formulated below (via the relative slenderness, $\overline{\lambda}$).

$$N_{cr} = \frac{\pi^2 EI_y}{L^2} + \frac{L^2 c}{\pi^2} \qquad \text{if} \qquad L < \pi \sqrt[4]{EI_y/c} \tag{4.10}$$

$$N_{cr} = 2\sqrt{cEI_y}\pi^2 \qquad \text{if} \qquad L \leq \pi \sqrt[4]{EI_y/c} \tag{4.11}$$

with $c = c_{multi} = \frac{8{,}9Et^3}{b^3}$ for a multi-stiffened plate with opened stiffeners and small torsional stiffness.

The effective plating thickness due to local buckling was smaller than the HAZ thickness, thus $t_{p,eff} = 3.71$ mm was used for the whole plate. The web is an internal part due to the flange, and the flange is an outstand. Outstands are defined as class 4 at an lower slenderness ratio, than class 4. If the flange was 4 mm thick, the web would be 72 mm high and the web would be required to be thinner than 3.92 mm to be considered class 4. If the web is 8 mm thick, the flanges outstand width is 21 mm. In that case the flange thickness would have to be less than 3.43 mm to be considered class 4. The web did however have a 30 mm HAZ, which was reduced $\rho_{c,6082,haz} = 0.48$ and thus $t_{w,haz,eff,} = 3.84$ mm. The plate would have had to be thicker than 12.89 mm to not have been considered class 4.

4.5.2 Plate under Uniform Compression

The resistance of the P6-Sf8-T10 panel may also be estimated with the assumption that the stiffeners, and especially the girders, are strong enough for the critical capacity to be similar to the capacity of the plating in between. For this model a plate with a width of 232 mm (=240-t_w)and length of 950 mm (=960-t_g) and a thickness $t_p = 6$ mm is analysed.

The *EC9* formulation for buckling of plates is valid for plates with uniform thickness and that are supported along all four edges. The support conditions may be hinged, elastically restrained or fixed, and it may be free along the long edge.

Again, the effective plating thickness was smaller than the HAZ thickness, and $t_{p,eff} = 3.71$ mm was used for the whole plate. The resulting buckling capacity was $\sigma_{plate} = 154.39$.

Some notes

rho haz is least favorable for approx tp above 6.05 mm. Plate must be above 13.3 mm thick to be class 3.

Internal web has reduced thickness 0.99 for tf=tw=4mm

4.5.3 Resistance Under Combined Loading

The resistance of the plate in combined loading conditions can be calculated by separating the loading into pure load cases described in the previous subsections and combining them in the interaction Equation (4.12). N_{Ed}, M_{Ed} and V_{Ed} are the applied axial, moment and shear loads, respectively. The coincident shear force may be ignored if it does not exceed $0.5V_{Rd}$.

$$\frac{N_{Ed}}{N_{c,Rd}} + \frac{M_{Ed}}{M_{c,Rd}} + \left(\frac{2V_{Ed}}{V_{c,Rd}} - 1\right)^2 \leq 1 \tag{4.12}$$

4.6 DNV GL's RU-HSLC

RU-HSLC was first published in December 2015 and is DNV GL's rules for classification of high speed and light crafts. Content from *RU-SHIP*, i.e. rules for materials and welding, is reused for the convenience of both DNV GL and ship builders. The following review will focus on aspects relevant to ultimate strength and buckling of stiffened aluminium panels located at the ship bottom. There may be simplifications of the regulation in this review without prior warning. The most relevant part for the review is *RU-HSLC pt. 3 ch. 3 - Hull structural design, aluminium*. Its formulas are dependent on the design loads established in *RU-HSLC pt.3 ch.1 - Design principles, design loads* and the aluminium material properties established in *RU-SHIP pt2. ch.2 - Metallic materials*. In addition, *RU-HSLC pt.3 ch.3* refers to the DNV GL's class guide on buckling, *DNVGL-CG-0128*, as well as the general ship regulation, *RU-Ship pt.1 ch.1*.

4.6.1 Class notations in brief

A light craft(LC) is defined to be a craft with a full load displacement not more than $\Delta = (0.13BL)^{1.5}$ tonnes. A high speed light craft (HSLC) is additionally required to be capable of a maximum speed equal to or exceeding $V = 7.16\Delta^{0.1667}$ knots. In addition to the main class features of *RU-HSLC* , all crafts have one of the ship type notations (Pt.1 Ch.2 Sec.); *Passenger craft, Car ferry, Cargo craft, Crew boats, Patrol boats, Small service craft, Naval and naval support vessels* and *Naval landing craft*. Some aspects of the design process is influenced by the ship type notation, including minimum wave conditions, in H_s, the ship shall be capable to operate during at maximum speed while fully loaded. Another important notation is the service area notation (Pt.1 Ch.2 Sec.5) which specifies how many nautical miles from land or safe anchorage a vessel is allowed to operate. The service area notation are denoted *R0* to *R6*. *R6* represents the most restricted service area and is limited to enclosed waters such as fjords, ports, rivers and lakes.

4.6.2 Aluminium Material Properties in HSLC

All aluminium alloys used in relation to *RU-HSLC* are defined in *RU-SHIP pt.3 ch.3* in which Young's modulus of elasticity is given as $E = 70000\ \mathrm{N/mm^2}$ and Poisson's ratio is given as $\nu = 0.33$[3]. The material factor f_1 (*RU-HSLC p3. ch.3*) is dependent on profile-type, grade, temper, welding and loading conditions, and it is used to determine the allowable stress level. f_1 may be applied when:

$$f_1 = \sigma_f / 240 \tag{4.13}$$

where
σ_f = yield stress and shall not be taken greater than 70% of the ultimate tensile strength.

4.6.3 Allowable stresses

The equivalent stress (von Mises) is defined as:

$$\sigma_e = \sqrt{\sigma_x^2 + \sigma_y^2 - \sigma_x \sigma_y + 3\tau^2}, \qquad \text{where} \tag{4.14}$$

σ_x = total normal stress in x-direction,
σ_y = total normal stress in y-direction, and
τ = total shear stress in the xy-plane.

Allowable equivalent nominal stresses referred to 20 year conditions in $\mathrm{N/mm^2}$. σ_f is yield stress of the material an. For aluminium and extreme 20 year loads, the allowable equivalent plastic strain corresponding to linear peak stress is $\sigma_e = 300 f_1$.

4.7 Design Loads

The design loads, defined in *RU-HSLC pt.3 ch.1*, are determined on the basis of vessel class, service restrictions, operating speed, hull shape and so on. In the following the design loads from transverse bending moments and loads, sea pressure, slamming loads and deck loads are examined. This examination of the code, will focus on panel strength of a bottom panel. This description is simplified and and is only meant to give some insight into the rules. The design loads are based on operational parameters that give restrictions to operating speed versus significant wave height.

[3] A notable difference is that Poisson's ratio is given as $\nu = 0.3$ in *Eurocode 9*

4.7.1 Slamming Pressure on Bottom

The design slamming pressure on the bottom of a craft with speed $V/\sqrt{L} \geq 3$ shall be taken as [*3.2.1*]:

$$p_{sl} = \frac{a_{CG}\,\Delta}{0.14 A_{ref}} K_{red}\, K_l\, K_\beta \qquad [\text{kN/m}^2] \tag{4.15}$$

Where:
a_{cg} [m/s^2] is the design vertical acceleration,
Δ [tonne] is the fully loaded displacement,
A_{ref} [m^2] is the impact reference area (=0.7 Δ/T),
K_{red} [-] is the design load area reduction factor,
K_l [-] is the longitudinal distribution factor ($0.5 \leq K_l \leq 1.0$),
K_β [-] is the correction factor for local deadrise angle.

4.7.2 Pitching Slamming Pressure on Bottom

All crafts shall be designed for a pitching slamming pressure on the bottom given as [*3.2.5*]:

$$P_{sl} = \frac{21}{\tan(\beta_x)}\, k_a\, k_b\, C_w\, (1 - \frac{20 T_{FP}}{L})\, (\frac{0.3}{A})^{0.3} \qquad [\text{kN/m}^2] \tag{4.16}$$

where:
k_a and k_b [-] are factors dependent on the structural element type ($\leq$ 1.0),

T_{FP} [m] is defined in figureXX,
A [m^2] is the design load area for the element type ($A \geq 0.002\,\Delta/T$).

Sea Pressure

The sea pressure for a load point below design waterline shall be taken as [*3.5.1*]:

$$p = a \left(10\, h_0 + \left(k_s - 1.5\, \frac{h_o}{T}\right) C_W\right) \qquad [\text{kN/m}^2] \tag{4.17}$$

where:
a [-]is a load intensity factor (=1 for bottom),
k_s equals 7.5 aft of amidships or $5/C_B$ forward of FP,
h_0 [m] is the vertical distance between the waterline at draught T to the load point,
C_w [m] is the wave coefficient which equals 0.08 $L\, f_r$ for $L \leq$ 100m, where f_r ($0.4 \leq f_r \leq 1.0$) is the class notation reduction factor of C_w.

In addition to the sea pressure given by equation 4.17, there are minimum design sea pressure values given for different locations of the vessel and which are dependent

on the restricted service class notations. For example, the minimum sea pressure for the bottom of a vessel rated for unrestricted service (*R0*) is 6.5 kN/m^2, while it is 5.0 kN/m^2 for vessels rated *R1* to *R3* and 3.0 kN/m^2 for vessels rated *R4* to *R6*.

Hull Girder Loads

The longitudinal hull girder loads, defined in *RU-HSLC Pt.3 Ch.1 Sec.4*, are to be determined on the basis of the high speed mode cases crest landing and hollow landing, as well as displacement mode cases caused by the vessel's motion in a seaway. Crest landing refers to bottom slamming around the midship area, inducing hogging moment, while hollow landing refers to bottom slamming around the fore and aft areas, inducing sagging moment. For both cases an impact slamming area and longitudinal midship bending moment are defined. Crest landings (4.18) and hollow landings (4.19) induce longitudinal midship bending moments which are defined as

$$M_B = \frac{\Delta}{2}\left(g_0 + a_{cg}\right)\left(e_w - \frac{l_s}{4}\right) \qquad \text{[kNm]} \qquad (4.18)$$

$$M_B = \frac{\Delta}{2}\left(g_0 + a_{cg}\right)(e_r - e_w) \qquad \text{[kNm]} \qquad (4.19)$$

Where:
g_0 [m/s^2] and a_{cg} [m/s^2] denotes the acceleration of gravity and the design vertical acceleration at longitudinal centre of gravitation, respectively,
l_s [m] is the longitudinal extension of the slamming reference area.
A simplified explanation of e_w [m] and e_r [m] is that e_w is the mean distance from vessel centre to fore and aft centre, while e_r is the mean distance from vessel centre to the slamming area. e_w is approximately $0.25L$, while $(e_r - e_w)$ and $(e_w - l_s/4)$ should not be taken less than $0.04L$.
In addition, the distribution factor k_m [-] applies to both bending moments, such that $M = k_m M_B$ shall be taken as the minimum bending moment at any arbitrary position along the length of the vessel[4]

Hull Girder Sea Loads

For hogging and sagging bending moments the longitudinal hull bending moments shall not be taken less than [*1.5.1*]

$$M_{tot} = M_{sw} + M_w \qquad \text{[kNm]} \qquad (4.20)$$

[4]This requirement was amended to Ch.1 Sec.4 [1.2.3] and [1.3.3] in October 2020 and entered into force on 01-01-2021. In the two previous editions, a similar requirement, Ch.1 Sec.4 [1.5.2], only applied to bending moments, M_{tot}, calculated as the sum of bending moments from still water and wave conditions.

where:
M_{sw} is the still water bending moment in the most unfavourable condition,
M_w is the wave bending moment amidships.

If the moments of a monohull craft are unknown, the hogging bending moment can be taken as

$$M_{tot} = M_{sw} + M_w = 0.11\, C_W\, L^2\, B\, C_B + 0.19\, C_W\, L^2\, B\, C_B \tag{4.21}$$

and the sagging bending moment can be taken as

$$M_{tot} = M_{sw} + M_w = 0 + 0.14\, C_W\, L^2\, B\, (C_B + 0.7) \tag{4.22}$$

If the still water moment S_{sw} is a hogging moment, 50% of it can be deducted from the design sagging moment.

Shear

The vertical hull girder shear force shall be calculated from the hull girder bending moments and is taken as [*1.6.1*]:

$$Q_b = \frac{M_b}{0.25L} \qquad [\text{kN}] \tag{4.23}$$

The distribution of the shear forces along the hull girder shall not be taken less than

$$Q_x = K_q Q_b \qquad [\text{kN}] \tag{4.24}$$

where:
k_q is the shear distribution factor in figurexx.

4.7.3 Longitudinal and Transverse Loads

The longitudinal loads to be considered are induced from inertia due to surge acceleration a_1, thrust and sea end pressures. The transverse loads induced from inertia due to transverse acceleration shall also be considered.

Table 4.3: Allowable bending stresses in plates and stiffeners[N/mm^2]

Item	Plate	Stiffener
Bottom and flat cross structure, slamming load	200 f_1	180 f_1
Bottom and flat cross structure, sea load	180 f_1	160 f_1
Side and Deck	180 f_1	160 f_1
Bulkhead, collision	180 f_1	160 f_1
Superstructure/deckhouse front	160 f_1	140 f_1
Bulkhead, watertight	220 f_1	200 f_1
Tank bulkhead	180 f_1	160 f_1

4.8 Structural Requirements

In the following, the most relevant requirements for stiffeners, plates, frames and hull girders from DNV GL's *RU-HSLC Pt. 3 Ch. 3* are assessed. An important factor that is applied throughout the *RU-HSLC* rules is the material factor f_1, which varies with alloy, temper and fabrication process.

Plating and Stiffeners

The requirements for local strength and thickness of plates and stiffeners for high speed and light aluminium crafts are given in *RU-HSLC Pt3. Ch.3 Sec. 5* The maximum allowable bending stresses, measured by the equivalent stress, are given in table 4.3.

(Buckling strength requirements are related to longitudinal hull girder stresses. Panels subjected to other compressive, shear or biaxial stresses will be specially considered.)

The minimum thickness of any structural member is [2.1.1]

$$t = \frac{t_0 + kL}{\sqrt{f}} \frac{S}{S_R} \,[\text{mm}] \tag{4.25}$$

where $f = \sigma_f / 240\,[\text{N/mm}^2]$, S [m] is the actual stiffener spacing and S_R=2(100+ L)/1000 [m] is the basic stiffener spacing which is limited such that $0.5 \leq S/S_R \leq 1.0$.

t_0 and k are parameters for each specific part of the vessel. t_0 ranges from 1.0 in superstructure to 10.0 in shell plating of bottom aft in way of rudder, shaft brackets. It is 4.0 in bottom shell below water line. k ranges from 0 to 0.1 in shell plating of bottom aft in way of rudder, shaft brackets. It is 0.03 in bottom shell plating.

Thickness of Plates Subjected to Lateral Pressure

The general requirement for thickness of plating subject to lateral pressure is given by Ch. 3 Sec.5 [2.2]

$$t = \frac{s\sqrt{Cp}}{\sqrt{\sigma}}, \text{[mm]} \tag{4.26}$$

where C (=s/l) is the correction factor for aspect ratio and degree of fixation. The requirement for a plate field clamped along all edges and with an aspect ratio $\leq$ 0.5 is

$$t = \frac{22.4s\sqrt{p}}{\sqrt{\sigma}}, \text{(mm)} \tag{4.27}$$

The bottom plating should be strengthened to withstand slamming, thus the minimum thickness of the bottom plating shall not be less than

$$t = \frac{22.4k_r k_a s\sqrt{P_{sl}}}{\sigma_{sl}}[mm] \tag{4.28}$$

, where k_a is a correction factor for aspect ratio of plate field, k_r is the curved plate correction factor, P_{sl} is the slamming pressure given in Ch.1 Sec.3 and described in sectionxx and $\sigma_{sl} = 200f_1$ [N/mm^2].

Section Modulus of Stiffeners

The strength of the stiffeners is defined by their section modulus. The section modulus of longitudinals, beams and other stiffeners subjected to lateral pressure should not be less than [Ch.3 Sec. 5 3.1.1]

$$Z = \frac{ml^2sp}{\sigma} \text{ (cm}^3\text{)}, \tag{4.29}$$

where m is a bending factor dependent on the degree of end constraints and type of loading. The longitudinal or transverse stiffeners supporting the bottom plating must withstand slamming loads and for these the section modulus should not be less than [3.1.1]

$$Z = \frac{ml^2sp_{sl}}{\sigma_{sl}} \text{ (cm}^3\text{)}, \tag{4.30}$$

where $m = 85$ for continuous longitudinal members and $m = 100$ for transverse members. The shear area is not to be less than [3.2.1]

$$A_S = \frac{6.7(l-s)sp_{sl}}{\tau_{sl}} \text{ (cm}^2\text{)}, \tag{4.31}$$

where $\tau_{sl} = 90f_1$.

4.8.1 DNV GL Buckling Regulation

DNV GL's buckling regulation is defined in *CG-0128*. The safety format in the rules is written in the form $\eta \leq \eta_{all}$. This means that the actual utilization factor η is not allowed to exceed any of the allowable levels given in the rules. For stiffened panels the buckling utilization factor is 0.8 in a static load condition, while it is 1.0 for dynamic loading conditions as well as accidental design scenarios. For comparison, it is in the range $0.65 - 0.9$ for struts, pillars, cross-ties, corrugated bulkheads, etc. In general are large elastic deflections of local plate elements in ship structures not deemed critical, as long as its functional and operational requirements are not jeopardized. This is due to the redundancy characteristics of plate buckling.

Plate Limit State

The utilization factor is defined as $\eta = \frac{1}{\gamma_c}$. The following interaction formula describes the plate limit state[*2.2.1*];

$$\left(\frac{\gamma_{c1}\sigma_x S}{\sigma_{cx}{}'}\right)^{e_0} - B\left(\frac{\gamma_{c1}\sigma_x S}{\sigma_{cx}{}'}\right)^{\frac{e_0}{2}}\left(\frac{\gamma_{c1}\sigma_y S}{\sigma_{cy}{}'}\right)^{\frac{e_0}{2}} + \left(\frac{\gamma_{c1}\sigma_y S}{\sigma_{cy}{}'}\right)^{e_0} + \left(\frac{\gamma_{c1}|\tau|\, S}{\tau_c{}'}\right)^{e_0} = 1 \tag{4.32}$$

$$\left(\frac{\gamma_{c2}\sigma_x S}{\sigma'_{cx}}\right)^{(2/\beta_p^{0.25})} + \left(\frac{\gamma_{c2}|\tau|S}{\tau'_c}\right)^{(2/\beta_p^{0.25})} = 1 \qquad \text{for } \sigma_x \geq 0 \tag{4.33}$$

$$\left(\frac{\gamma_{c3}\sigma_x S}{\sigma'_{cy}}\right)^{(2/\beta_p^{0.25})} + \left(\frac{\gamma_{c3}|\tau|S}{\tau'_c}\right)^{(2/\beta_p^{0.25})} = 1 \qquad \text{for } \sigma_y \geq 0 \tag{4.34}$$

$$\frac{\gamma_{c4}|\tau|S}{\tau'_c} = 1 \tag{4.35}$$

(4.36)

With
$$\gamma_c = \min(\gamma_{c1}, \gamma_{c2}, \gamma_{c3}, \gamma_{c4}) \tag{4.37}$$

and
$$\beta_p = \max\left(\frac{b}{t_p}\sqrt{\frac{R_{eH\_P}}{E}}\ ,\ 1.0\right) \tag{4.38}$$

Where:
σ_x, σ_y and τ [N/mm^2] denotes the applied normal stresses and shear stress to the plate,
σ'_{cx},σ'_{cy} and τ'_c [N/mm^2] denote the ultimate buckling normal and shear stresses,
γ_{c1}, γ_{c2}, γ_{c3} and γ_{c4} denotes the stress multiplier factors at failure for each of the above different limit states,
B and e_0 are coefficients given in tablex,
β_p denotes the plate slenderness parameter,
α is the plate panel aspect ratio (=a/b),

Table 4.4: Definitions of coefficients B and e_0

Applied Stress	B	e_0
$\sigma_x \geq 0$ and $\sigma_y \geq 0$	0.7 - $0.3\beta_p/\alpha$	$2/\beta_p^{0.25}$
$\sigma_x \leq 0$ or $\sigma_y \leq 0$	1.0	2.0

b [mm]denotes the short length of the plate,
t_p [mm] denotes the net thickness of the plate, and
R_{eH_p}[N/mm^2] denotes the specified minimum yield strength of the plate.

For a stiffened panel with a T-stiffeners fixed at both ends and $t_w/t_p \geq 1$, the correction factor F_{long}=1.3.

4.8.2 Elastic Buckling of Stiffened Panels

HSLC Pt.3 Ch3. Sec.10
The ideal elastic buckling stress,$\sigma_{el,plate}$ off a plate under uniform uni-axial comression can be taken as:

$$\sigma_{el,plate} = 3.6\,E(\frac{t}{s}) \qquad [\text{N/mm}^2] \tag{4.39}$$

Elastic buckling of the plating between stiffners may be allowed under the following conditions:

- $\sigma_{el,plate} = \sigma_{c,plate}$
- $\eta_{stiff}\sigma_{c,stiff} > \eta_{plate}\sigma_{el,plate}$ in compression
- there are no functional requirements limiting the deflectinos
- extreme loads are used in the calculations

Hull Section Modulus Requirement

The hull section modulus is defined in *sec.4 [2.1]* as

$$Z = \frac{M}{\sigma}10^3 \qquad [\text{cm}^3], \tag{4.40}$$

where $\sigma = 175 f_1$ and M [kNm] is the longitudinal midship bending moment from *Pt.3 Ch.1 Sec.4*, which are described in section 4.7.2.

4.9 HSLC Uni-axial Compression Buckling

For a plating in uni-axial compression the ideal elastic buckling stress is given as:

$$\sigma_{el} = 0.9kE\left(\frac{t}{1000s}\right)^2 \qquad [\text{N/mm}^2] \tag{4.41}$$

If the plating is longitudinally stiffened and the compressive forces changes linearly over the cross-section, k equals k_l and is given as:

$$k_l = \frac{8.4}{\psi + 1.1} \qquad \text{for } (0 \leq \psi \leq 1) \tag{4.42}$$

Where ψ is the ratio between the smaller and the larger compressive stress assuming linear variation.

Chapter 5

Abaqus and Finite Element Theory

The following chapter will contain FEM theory.

5.1 Nonlinear Finite Element Method

The Finite Element Method (FEM) is a numerical method for solving partial differential equations of a domain by subdivision into smaller and simpler parts. It was originally developed to solve complex elasticity problems within civil and aeronautical engineering. Today finite element analysis (FEA) and nonlinear finite element analysis (NFEA) is used in many engineering disciplines and some of its applicability includes:

- structural elasticity analysis,
- heat flow analysis,
- fluid flow analysis,
- electromagnetic field analysis, and
- fatigue and fracture mechanics.

5.1.1 Linear and nonlinear analysis

In linear analysis the relation between applied forces and deformations are assumed to be linear. This assumption may be valid for if the material law is linear elastic and the displacements are relatively small. In linear analysis the equilibrium and compatibility equations may be based on the undeformed geometry. Thus, the structures stiffness matrix remains constant and the computational effort required is relatively low. The assumptions of linear behaviour does however not hold true for many problems. Nonlinear behaviour may originate from large deformations, material nonlinearity and boundary conditions, i.e. contact problems. In nonlinear analysis the stiffness matrix changes during the analysis.

Some of the advantages of the finite element method include[21]:

- No geometrical limitations within 3D space.
- The material properties may be anisotropic, time and/or temperature dependent and the assembly may consist of parts with different material properties.
- A large variety of boundary and loading conditions are possible.
- The element type and finite element mesh size may vary across a part or assembly.

5.2 Material Nonlinearity

Nonlinear material behaviour refers to stress-strain relations that can not be adequately described linearly. Solids typically deform linear elastically at low strain levels. That is, it may be formulated $\sigma = E\epsilon$ and the material will return to its original shape when loading is removed.

At higher stress-strain levels, most solids exhibit nonlinear stress-strain behaviour. In metals, nonlinear behaviour often coincides with stress levels above yield and plastic deformation. Some solids, including aluminium, exhibit nonlinear stress-strain relations much earlier than yield. Nonlinear effects may also include viscosity, i.e. time-dependent behaviour, and thermal expansion.

5.3 Geometrical Nonlinearity

Geometrical nonlinearity refers to nonlinear effects associated with large deformations of the initial geometry. This is accounted for by allowing the local material direction to rotate with the deformation of each element. Another nonlinear effect of large deformation is that the stress state must be described by true stress-strain relations preserve accuracy.

5.3.1 True strain-stress relations

Structural materials are typically listed by engineering stress-strain parameters, but many FEA programs, including Abaqus, require true stress-strain data. Engineering values may easily be transformed to true values by the following formulas. These transformations from engineering to true stress-strain are only valid for incompressible materials, i.e. $A = A_0 \frac{l_0}{l}$, prior to necking[22]:

$$\epsilon_{Eng} = \frac{|l - l_0|}{l_0} \quad (5.1) \qquad \sigma_{Eng} = \frac{P}{A_0} \quad (5.2)$$

$$\epsilon_{True} = \ln\frac{l}{l_0} = \ln(1 + \sigma_{Eng}) \quad (5.3)$$

$$\sigma_{True} = \frac{P}{A} = \frac{P}{A_0}\frac{l}{l_0} = \sigma_{Eng}(1 + \epsilon_{True}) \quad (5.4)$$

$$(5.5)$$

5.4 Abaqus

Abaqus was used to perform ultimate axial compressive strength analyses of a stiffened panel.

5.4.1 Elements

A fundamental aspect of FEA is the element description which determine the behaviour of the model. The five main aspects that characterize the element behaviour of an Abaqus element are:

- Element family
- Number of nodes
- Degrees of freedom
- Formulation
- Integration

Elements Characteristics

Abaqus[22] has a variety of element families, including shell, continuum, membrane, beam, truss and connector elements. A main difference between the families is whether the elements of a family are one, two or three dimensional. A fundamental aspect of any element is the number of nodes the element has, and which degrees of freedom those nodes have. Displacements, rotations or any other variable, i.e. temperature, are calculated at the nodes. At any other point in the element the variables are obtained by interpolation of the nodal variables. All elements have nodes at their corners, but elements may also have edge nodes. The elements that only have corner nodes are often called linear elements, as only linear interpolation is possible to obtain values at any other point in the element. With an edge node between two corner nodes, second- order interpolation is possible between those nodes.

The FE problem may be interpreted and assessed using different mathematical theories and physical assumptions, which in Abaqus are referred to as different formulations. Example given, a beam may be analysed using either Euler-Bernoulli beam theory or Timoshenko beam theory. Integration refers to whether full or reduced integration is used to establish the stiffness matrices. In some cases reduced

integration, meaning integration with a quadrature rule of less than full order, may lead to improved accuracy because it softens the element and reduced computational time. The downside, however, is that if the strains vanish at all Gauss points during a non-rigid deformation mode, the strain energy will integrate to zero. This leads to modes with no physical basis that are called hourglass-modes (or spurious-modes or zero-energy-modes).

Shell Elements

There are three different formulations for three-dimensional shell elements as described by the Abaqus documentation [22]: General-purpose, Thin and Thick shells. The thin shell elements are based on Kirchhoff's classical plate theory, in which transverse shear flexibility is negligible and the shell normal is assumed to remain orthogonal to the shell reference surface. The thick shell elements are based on Mindlin-Reissner theory, in which transverse shear flexibility and second-order interpolation is implemented. There may be specific cases where thin or thick shell elements may give enhanced performance, but the general-purpose shell elements are suggested by Abaqus to be the first choice. All three of them can provide for arbitrarily large rotations, but the thin and thick shell elements can only handle small strains and assumes fixed shell thickness, while the general-purpose shell elements provide for finite strains and allows the thickness to change with the element deformation. The general-purpose shell element contains both thick and thin behaviour, and adjusts its behaviour towards thick or thin formulation in accordance with its thickness. The result is an adaptable shell element that provide robust and accurate solutions to most applications[22].

Chen [23] performed an element sensitivity study of S4, S4R, S4R5, S8R and S8R5 to determine which shell element would be the best choice for buckling analysis of stiffened aluminium panels. The S4R, which is a general-purpose 4-node, doubly curved quadrilateral with large-strain formulation and reduced integration, was chosen. The results of S4 and S4R (both general-purpose) where almost identical, but S4R was computationally 67% faster due to reduced integration. The thick S8R and S8R5 converged quickest, but their thickness is fixed, thus their stress-strains are not based on true stress-strains. The same applies to the thin S4R5.

5.5 Linear Eigenvalue Buckling Analysis by Abaqus

The result of a Linear eigenvalue buckling analysis are eigenvalues $omega_i$ and associated deformation shapes (i.e. eigenvectors v_i^M). The first eigenvalue may be used to predict the theoretical critical buckling load, computed as the initial load times the eigenvalue, but this method tend s to over-predict the true buckling load[22]. Usually the aim of the linear eigenvalue buckling analysis is to implement the obtained deformation shapes as initial distortions into another structural analysis.

The eigenvalue problem, as described by the *Abaqus documentation* [22], is formulated as:

$$(K_0^{MN} + \omega_i K_\Delta^{MN}) v_i^M = 0, \tag{5.6}$$

Where: K_0^{NM} is the stiffness matrix of the base state, which includes the effects of the preloads, P^N,
K_Δ^{NM} is the load stiffness matrix due to the incremental loading pattern,Q^N,
ω_i are the eigenvalue vector,
v_i^M are the buckling mode shapes (eigenvectors). M and N refers to degrees of freedom of the whole model and i refers to the ith buckling mode. The first eigenmode is usually of most interest, as its associated with the deformation of least resistance.

5.6 Riks Method

During buckling or collapse of stiff structures the load-displacement response may show a negative stiffness as the structure releases strain energy to remain in equilibrium[22]. Many FEA programs can not solve these unstable behaviours and would crash. The reason is that that most commercial FEA programs, including the static analysis in Abaqus, uses Newton's method to solve the nonlinear equilibrium equations, written as the virtual work principle[22]. There are several methods to solve such problems. Load or displacement control may be used to stabilize the snaps, and the inertia effects of a snap may be modeled in a dynamic analysis after the static analysis is terminated. The structure may also be stabilized with dash pots[22].

Why Newton's method fails[24]

Solving the nonlinear equilibrium equations may be thought of as finding a continuous path in the multidimensional load-displacement space ($\boldsymbol{\lambda} - \boldsymbol{u}$). The path starts at some initial equilibrium point ($\boldsymbol{\lambda_o}, \boldsymbol{u_o}$) and next deformation point ($\boldsymbol{u_o} + \boldsymbol{\Delta u_o}$) may be found by increasing the loading by a small load increment $\boldsymbol{\Delta\lambda}$ and solving the equilibrium equations. Newton's method is fast, but it fails when the tangent stiffness reaches zero, because no stable points can be found with loading greater than the limit point[24]. There are methods to improve the stability, see Figure 5.1 such as and load control and displacement control, which may allow Snap-Trough and Snap-Back, respectively.

5.6.1 The Modified Riks Method by Abaqus

If the load increments may be described by a single parameter and the response is reasonably smooth, the modified Riks method can be used to analyse unstable problems[22]. The load increment is determined by the load proportionality factor λ_R. Instead of solving the equations by either load control or displacement control, the load and displacement are combined to one variable, the arc length. This

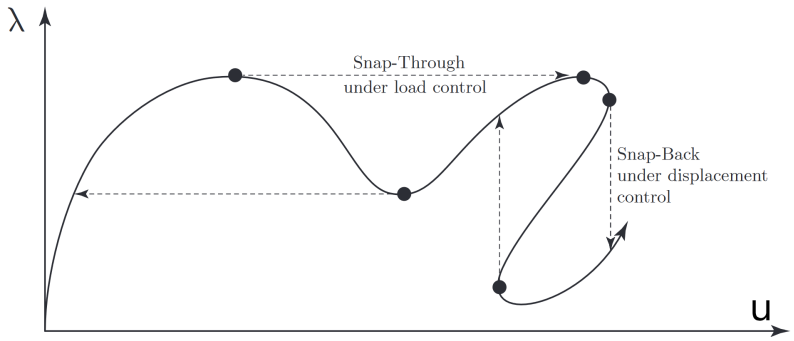

Figure 5.1: Illustration of Snap-Through and Snap-Back for static analysis[24]

method can be thought of as finding the continuous path of points ($\boldsymbol{\lambda}$, $\boldsymbol{u}$) that satisfy the equilibrium equations by searching the multidimensional load-displacement space with the arc length as radius[24]. When a new equilibrium point is found the analysis is progressed from this point. A drawback of this method is that the circle (or sphere) intersects with the path at two points. An Riks algorithm may sometimes struggle to distinguish which set of points ($\boldsymbol{\lambda}$, $\boldsymbol{u}$) move the solution forward[24].

The modified riks algorithm as it is implemented in Abaqus inspired by the improvements suggested by Crisfield (1981) and others is described as follows[22]. From a stable, scaled, equilibrium point $(\widetilde{\boldsymbol{u}}, \boldsymbol{\lambda}_R, o)$, the tangent stiffness, $\boldsymbol{K_o^{MN}}$, is established and used to solve

$$\boldsymbol{K}_o^{MN}\, \boldsymbol{u}_o^M \;=\; \boldsymbol{P}^N \tag{5.7}$$

where: P^N is the loading pattern,
λ_R is the load magnitude parameter, also called load proportionality factor or LPF,
$\widetilde{\boldsymbol{u}}^N$ is the displacement at the time corresponding to λ_R,
$\lambda_R\, P^N$ is the actual load state,
$\overline{u}$ is the maximum absolute value of all displacement variables,
M and N are the degrees of freedom of the model.

$\overline{u}$ is used to scale the load-displacement space such that the dimensions have approximately the same maximum magnitude. The equilibrium points are described by ($\widetilde{\boldsymbol{u}}$, $\boldsymbol{\lambda}_R$)

The arc length Δl, in the scaled solution space is takens such that

$$\boldsymbol{\Delta\lambda}_{R,o}^2(\widetilde{\boldsymbol{u}}_o^N\,;\,1)(\widetilde{\boldsymbol{u}}_o^N\,;\,1) \;=\; \Delta l^2 \tag{5.8}$$

Chapter 6

Method - Ultimate Buckling Strength of a Stiffened Panel

A stiffened aluminium panel, which is meant model the bottom of a high speed and light craft, was analysed with respect to ultimate uni-axial compressive strength. The finite element program Abaqus was used to perform the analysis with the procedure listed below.

Ultimate strength analysis procedure:

- A representative FEM model was created with AA5083-H24 and AA6082-T6 material properties and HAZ extent according to *EC9*.
- A Linear Eigenvalue Buckling Analysis was performed and the deformation shape associated with the lowest eigenfrequency (mode 1) was implemented into the model to be used as initial imperfection for the next step.
- The modified Riks Method was used to analyse the ultimate strength and unstable collapse of the panel.
- Many panels with different thicknesses and HAZ patterns where analysed to compare the effects of the changes.

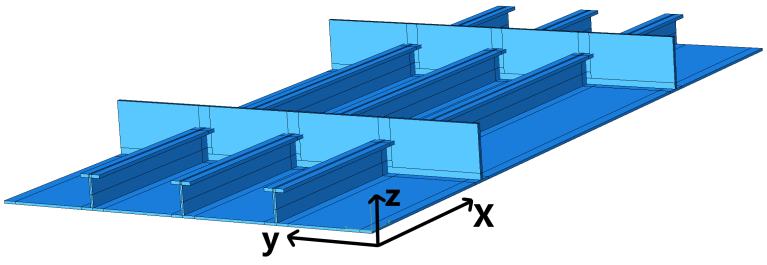

Figure 6.1: The stiffened aluminium panel modelled with Abaqus.

6.1 Assembly and Dimensions

The panel model, see Figure 6.1, consists of a plate that was stiffened with three longitudinal continuous T-stiffeners and two transverse girders. It was a two-span model, i.e. two transverse girders situated with the distances: 1/2 a + a + 1/2 a, were the girder distance, a, equals 960 mm. The stiffeners were situated like: b + b + b + b, were the stiffener distance, b, equals 240 mm. Thus the panel had a total length of 2a (=1920 mm) and a total width of 6b (=960 mm). The aspect ratio (a/b) of the entire model was 2, the aspect ratio of the plate-part between the girders was 1 and the aspect ratio of a plate-part between two girders and two stiffeners was 4. The entire model was created with shell-elements. The stiffeners and plate were created as one shell extrusion, while the transverse girder was created as a separate shell. Thus, the stiffener was appropriately connected to the plate by default, while the girders needed to be connected to the plate-stiffener part. In the following and through this entire thesis, the subscripts p, w, f, g denotes values for the plate, web, flange and girder, respectively. In addition, the x-, y- and z-axis always refers to those shown in Figure 6.1. That is, the x-axis was parallel with the stiffeners, the y-axis was parallel with the girder and the z-axis was parallel to the web.
In the base model, the plate thickness (t_p) was 6 mm, the web and flange thicknesses (t_w and t_f) were 8 mm and the girder thickness (t_g) was 10 mm. The other values for these thicknesses are listed in Table 6.1. All other dimensions, other than the thicknesses, were equal in all models. The flange width (b_f) was 50 mm, or 25 mm out on each side of the web. The stiffener height (h_{stiff}), including the flange thickness, was 76 mm. The girders were only modelled with a height (h_g) of 126.7 mm, but in a comparable ship hull they would likely have been twice as tall. This choice is explained in Section 8.1.3.

6.2 Material data and HAZ

In accordance with *RU-HSLC* recommendations, the parts that are in direct contact with sea water, i.e. the plate, is of a 5xxx alloy. The plate was modelled to be made of 5083-H24 in rolled condition, while the T-stiffeners and girders were modelled to be made of 6082-T6 extrusions. These alloys and tempers have been studied for similar purposes by Chen [23] and are realistic choices for a shipbuilder. The material parameters of the AA5083-H24-plate and AA6082-T6-extrusion were obtained from *Eurocode 9* . Both were modelled with a modulus of elasticity E = 70 000 MPa and a Poisson's ratio $\nu = 0.3$, in accordance with *EC9*. The alloy and temper properties that were obtained are listed in Section 6.2.

The yield criterion

The Von Mises yield criterion is used to assess critical points of the cross section and is formulated as follows.

Table 6.1: Dimensions of the panel. The subscripts p, w, f, g denotes values for the plate, web, flange and girder, respectively. The underlined values are the values of the base panel model, while the other are dimensions of alternative panels that were also analysed.

Properties	
E	70000 MPa
ν	0.3
Dimensions [mm]	
a	960
b	240
L_a	1920
L_b	960
t_p	5 | <u>6</u>
t_w,t_f	5|6|7|<u>8</u>
t_g	8|9|<u>10</u>
$h_{stiffener}$	76
h_g	126.7
b_{HAZ}	30
b_f	50

Material Data

The nonlinear stress-strain behaviour were implemented into Abaqus with the `*Plastic` - format as sets of true stress and true strain above the linear range. The strains where formulated as $\epsilon = \epsilon(\sigma)$ with the Ramberg-Osgood formulation in Excel. The Ramberg-Osgood formulation and true stress-strain transformations are described in Section 2.8 and Section 5.3.1. The obtained true stress-strain relations are plotted in Section 6.2.

Table 6.2: The obtained alloy properties from EC9. f_0 is the 0.2% proof strength and f_u is thee ultimate tensile strength.

Alloy-Temper (EN-AW)	**Thickness** [mm]	f_o [MPa]	f_u [MPa]	$f_{o,HAZ}$ [MPa] 1)	$\rho_{o,HAZ}$	$f_{u,HAZ}$ [MPa] 1)	$\rho_{u,HAZ}$	**BC** 2)	n_{RO} 3)
5083-H24 4)	≤ 25	250	340	155	0.62	275	0.81	A	14
6082-T6 5)	$5< t\leq 15$	260	310	125	0.48	185	0.6	A	25
1) Valid for MIG welding and thickness up to 15 mm.									
2) Buckling Class 3) Ramberg-Osgood exponent									
4) Wrought sheet, strip, plate									
5) Wrought, Extruded profile									

Heat Affected Zone

The panel was modelled with heat affected zones(HAZ) due to high temperature exposure from welding. The HAZ had an extent of $b_{HAZ} = 30$ mm from the welds, which is in accordance with *EC9* for MIG welding and average thicknesses of welded parts above 6 mm, see Section 4.4.2. The plate has HAZ where it is welded to the stiffeners, to the girders and along the long plate edges that are parallel to the stiffeners. The stiffener webs have HAZ where they are welded to the plate. The stiffener flanges and girders are not modelled with any HAZ. The HAZ patterns are shown in Figure 6.3 and Figure 6.4.

6.3 Meshing and Element types

The goal of the meshing process was to create a mesh that would yield accurate results at a relatively low computational cost. It was also important to avoid mesh-gaps, inconsistencies and large size changes. Triangular mesh-shapes were also avoided, as they may be induce excessive stiffness. Shell elements where chosen because they accurately describe bending and buckling behaviour of plates, see Section 5.4.1. The element selection process was heavily influenced by the convergence study performed by Qiaofeng Chen in his PhD-thesis [23]. The S4R-element, a general-purpose 4-node , doubly curved quadrilateral with large-strain formulation, was chosen for the whole model. The advantages of the S4R-element are discussed in Section 5.4.1, but in brief it it does not suffer from shear locking or unconstrained hour glass modes[22]. The default choice of five integration points across the thickness was chosen.

6.3.1 Panel Mesh

The smallest mesh-elements, had a size of 15 mm x 15 mm. The flange was meshed with one element on either side of the web and its mesh density along the x-direction matched that of the plate. Thus the flange elements were 25 mm x 30 mm and 25 mm x 15 mm. The web had 5 elements along its height, of which

two were in the 30 mm wide heat affected zone, and its width in the x-direction matched that of the plate. The plate had elements of size 15 mm in y-direction and 30 mm in x-direction, but this changed to 15 mm x 15 mm at a distance of 30 mm from the girder. It is generally advised to not have elements with large length to width ratios and the 15 mm x 30 mm elements are not recommended, especially not with the longest edge parallel to the main axis. This was assumed to not create significant errors, as the buckling and stress peaks were assumed to come between the girders. The parts of the structure that are out side of the two girders, are mostly there to provide accurate conditions for the panel-part between the girders.

6.3.2 Girder Mesh

The load transfer and stress levels in the girders were assumed to be very low. They were added to create realistic stiffness to the plate and stiffeners. For this reason, the aim of the girder meshing process was to create a mesh that would fit perfectly with the stiffener and plate mesh, but without unnecessary computational costs. The perfect fit was prioritized in order to use `TIE`-connection between the nodes. The chosen girder mesh, could potentially cause errors if the stress and strain levels were high in the girder, but this was not the case. The girder-panel connection is shown in Section 6.3.2 and the girder mesh is shown in Figure 6.7.

6.4 Boundary Conditions and Constraints

The boundary conditions must reflect the assumption that the panel is a part of the bottom of a ship hull. The boundary conditions are summarized in Table 6.3. The entire loaded short edge (edge set 2, including plate, web and flange edge) was forced to have equal x-direction movement. This was implemented by first creating a set of one node along the edge, `EdgeSingleNode` and a set of all the other nodes along the edge, `EdgeNodes`. Then the equation constraint was used to force the following equation on global degree of freedom 1, i.e. in the x direction:

```
EdgeNodes - EdgeSingleNode = 0
```

The other short edge (i.e. edge set 1) was restricted to not move in the x-direction. Both short edges were restricted to not rotate about Ryy and Rzz, where Ryy and Rzz denotes rotation about an axis parallel to the y- and z-axis, respectively. The midpoint of the plate of edge set 1 was also restricted to not move in the y-direction. This was the only y-direction rigidity of the entire model.

Long Plate Edges

The "neighbouring" panels must also be taken into account with the long edge boundary conditions. A reasonable assumption is that the long edges (edge set

3) are allowed to rotate(except Rxx) and translate, but that they have to remain straight. The Rxx rotation was fixed using the regular boundary condition module. The straight-line requirement was implemented by using the slider multi point constraint. The slider forces all nodes in a node set to remain on a straight line between two other nodes, which were the corner nodes. They are allowed to move freely along the line and to rotate (execept Rxx). The slider constraint is not supported by the graphical interface and has to be written directly into the keywords as follows:

```
**ConstraintName
*MPC
SLIDER, LeftEdgeNodes, CornerNodeLeftDown, CornerNodeLeftUp
SLIDER, RightEdgeNodes, CornerNodeRightDown, CornerNodeRightUp
```

Table 6.3: The boundary conditions of the panel. **Edge set 1:** Plate, web and flange edges at the fixed short end. **Edge set 2:** Plate, web and flange edge at loaded short side. **Edge set 3:** Plate edges of both long sides (not girder edges). **Edge set 5:** Top edges of transverse girders.

DOF's	Edge set 1	Edge set 2	Edge set 3	Edge set 5
x	Fixed	Kept straigth	1)	Free
y	Plate midpoint Fixed	Free	1)	Free
z	Free	Free	1)	Fixed
Rxx	Stiffener fixed	Stiffener fixed	Fixed	Free
Ryy	Fixed	Fixed	Free	Fixed
Rzz	Fixed	Fixed	Free	Free
1) SLIDER-MPC was used to restrict the long sides (Edge set 3) such that all the nodes along the edge where restricted to lie on a straight line between the respective corner nodes.				

Girders

The girders were connected to plate-stiffener part with the `Tie-connector`. The meshes were purposefully created to fit such that the girder nodes and the plate-stiffener nodes would coincide perfectly. The slave nodes on the plate and stiffener web were forced to follow the translation and rotation of the girder master nodes. Thus, this constraint models the plate and stiffener as being fixed to the girder, just as if they were welded.

Extra boundary condition for stiffener ends

The initial plan was to use equal boundary conditions for the stiffener edges as for the short plate edges. That is, Ryy and Rzz rotation should be restricted, and the

short edge without loads should not move in the x-direction. The short load edge should move in the x-direction as a straight line. However, initial investigations revealed some unwanted behaviour, were the torsional rotations as well as the y-direction movement of the stiffener ends were much larges than similar stiffener deformations between the girders. The part of the panel outside of the girders, as well as the girders themselves, are only modelled in an effort to create realistic responses of the panel area between the girders. In addition, the panel is modeled to be part of a larger hull. It is therefore reasonable to assume that the deformations of the stiffener ends should not be much larger than the deformations of the stiffener-parts that are in-between the girders. After extra stiffness was added to the stiffener edges(i.e. web and flange edges) in the form of restricting Rxx rotation, the deformations of the stiffener edges were more comparable to the deformations between the girders. All results are based on models with the extra stiffener-edge boundary condition.

6.5 Load Conditions

The panel was loaded in axial compression. The loads were applied as shell edge loads on the stiffener web, stiffener flange and plate edge. . The loads were always scaled to match the edge thickness such that the magnitude at any edge was equal to 100 times the edge thickness. For example, with the base case with $t_p = 6$ mm and $t_w = t_f = 8$ mm, the plate load magnitude was 600 pr unit undeformed length and the flange and web magnitude was 800 pr unit undeformed length. With this set-up the pressure at the panel edge was always 100 MPa and the total panel load was 100 MPa times the combined length of the panel edge (960 mm + 3*(76 mm + 50 mm) = 1338 mm).

6.6 Imperfections

All real-world structures have imperfections and FEA these have to be implemented manually. The imperfections may be implemented as the combination of harmonic deflections computed by elastic buckling theory, see Section 3.3, but in this project the imperfections where implemented as deformations based on eigenvalue analysis, see Section 5.5. The deformation shapes where obtained by using the `Linear Perturbation - Buckle` step on a copy of the model. The deformation shape has to be written to a file such that it can be used for other analysis steps. This is achieved by writing `*Node File U` into the keywords as follows:

```
* FIELD OUTPUT: F-Output-1,
*
Output, field, variable=PRESELECT
NODE FILE
U
```

The node file contains the new positions of all nodes, of which the most moved node is 1 unit away from its initial position. The first eigenvalue is associated with the shape of least buckling resistance given the initial loading pattern, thus it was used for ultimate buckling strength analysis. The first mode is shown in Section 6.3.2. A imperfection of $a/200 = 960\ \text{mm}/200 = 4.8$ mm was chosen in accordance with *Eurocode 9*. Sometimes it may be reasonable to implement the imperfection as a combination of multiple modes for realistic initial distortions of the whole model, but in this analysis the first mode was assumed to be enough. A risk of combining several modes is that the panel may have a higher buckling resistance with a combination, than with the first mode. It may also increase the likelihood of snapping. The same imperfection was implemented equally in all models by by writing the following into the key words:

```
*IMPERFECTION, FILE=job-file-name, STEP=step-number, NSET=whole-model-set
eigenmode-number, value-of-imperfection
```

6.7 Riks Analysis

The axial ultimate capacity was analysed with Riks modified method, which is described in Section 5.6. The panel was not pre-loaded, such that the ultimate capacity of the panel equals the applied loads times the load proportionality factor, also called LPF. The riks-step had to be edited such that it would run more iterations before it terminates. Riks was run several times with different thicknesses, as well as different HAZ patterns for the base model. The loads where adjusted between each run, such that the edge pressure would always be equal to 100 MPa pr unit length. For each run, a data set of the axial deformation of the mid node on the short load edge versus LPF was exported to excel and plotted.

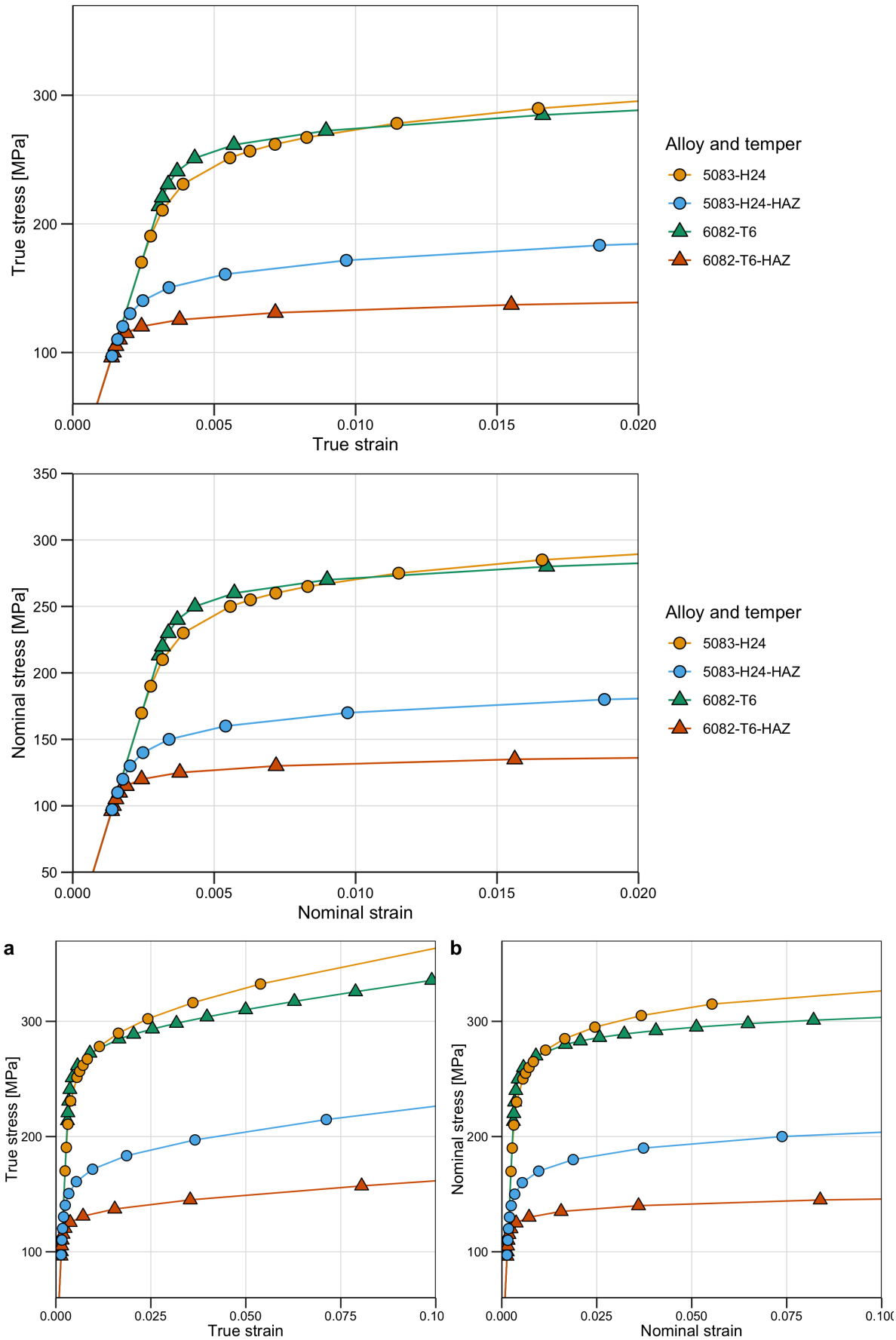

Figure 6.2: Stress-Strain relations of the chosen aluminium alloys. Each true stress-strain point represents a data point used in Abaqus, but with plastic strain.

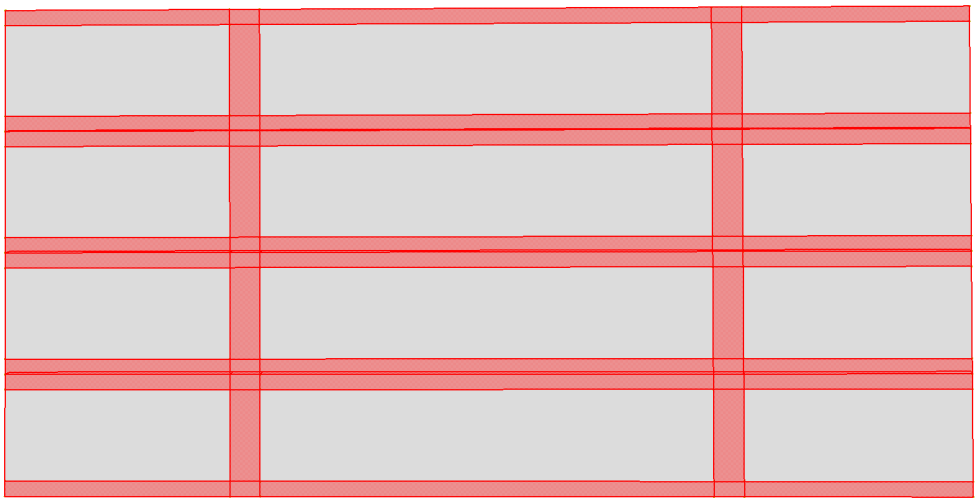

Figure 6.3: The HAZ pattern of the plate.

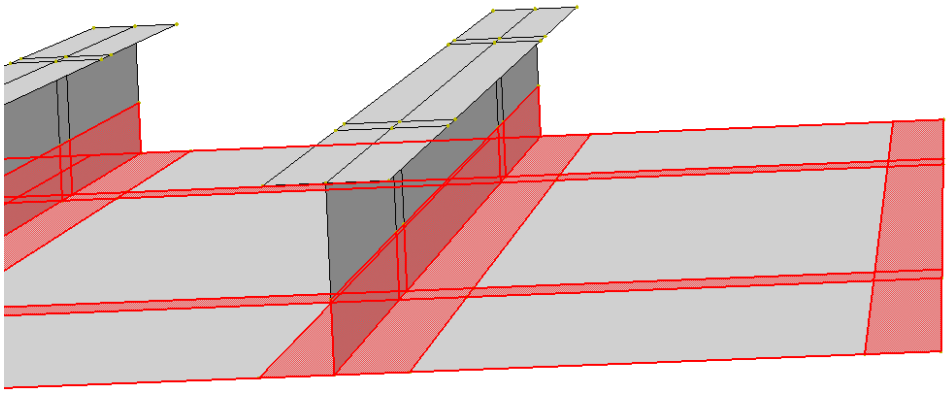

Figure 6.4: The HAZ pattern of the plate and the stiffener web.

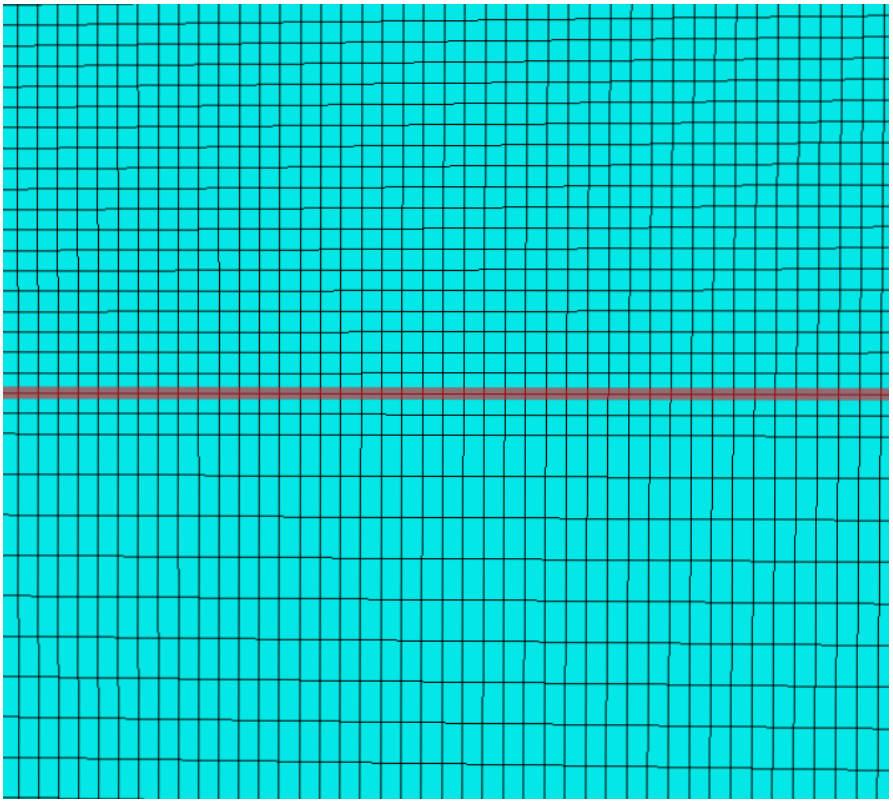

Figure 6.5: The stiffener mesh. There are 5 elements along the height(76 mm) of the stiffener. The flanges have one element on each side of the web. The density in the x-direction is similar to the plate mesh.

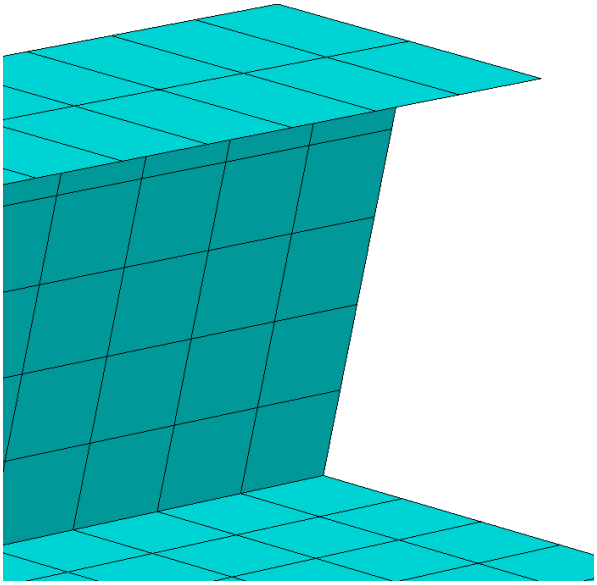

Figure 6.6: The plate mesh. The red line indicates the plate-girder connection. Note that there are two rows of 15 mm x 15 mm elements in the HAZ below the red line and between the girders. The other elements out side of the girders are 15 mm x 30 mm.

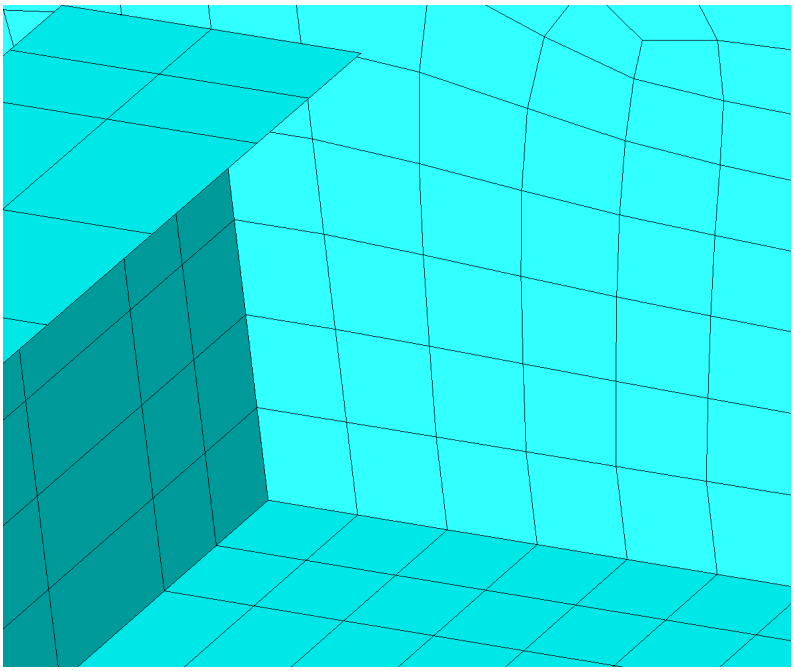

Figure 6.7: The girder mesh was created to fit perfectly with the plate and web mesh, such that the nodes would coincide. The stiffener comes into the frame from the left.

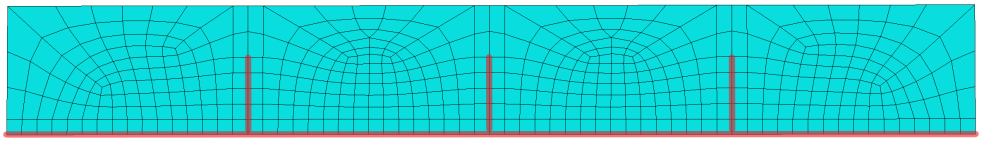

Figure 6.8: The transverse girder mesh. The red line shows the intersection with the plate and web.

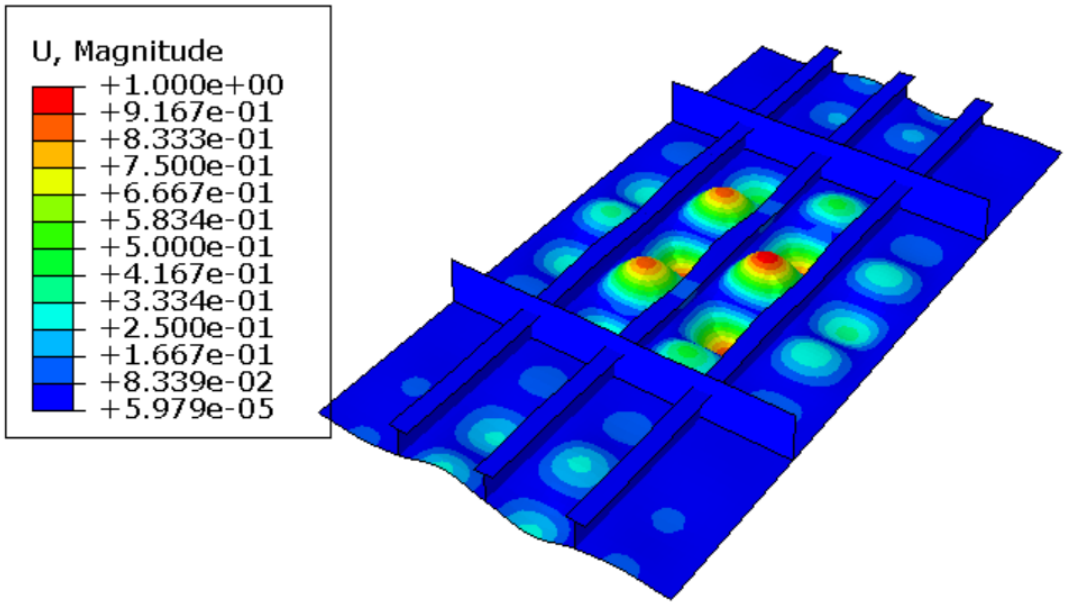

Figure 6.9: The deformation of mode 1 from eigenvalue buckling analysis. The deformations are scaled up 100 times.

Chapter 7

Results

In the following the results of the Abaqus FEA analysis and classification rule review will be presented.

7.1 Abaqus - Results

7.1.1 Change of Dimensions

The results of the Abaqus analysis are listed in Table 7.1 and the load-displacement curves are plotted in Section 7.2. The panel name Px-WFy-Tz refers to a panel with plate thickness t_p=x mm, web and flange thicknesses $t_w = t_f$ = y mm and transverse girder thickness t_g=z mm. In some plots S is used in stead off W. All FEA panels had a maximum capacity above 150 MPa. For the chosen changes of thicknesses, the ultimate capacity ranged from 161.32 MPa to 170.74 MP, with an average of 160.20 MPa. The difference in ultimate capacity was $\sim$ 9.4 MPa, or 5.87%. As expected, the ultimate axial capacity increased with larger cross-sectional area of the stiffener and plate. Decreasing the girder thickness, from 10 to 9 mm decreased the cross-sectional area and weight of the girder by 10%, with only a $\sim$ 0.1% decreased ultimate axial capacity.

Deformation

The base panel (P6-WF8-T10) had an axial deformation of 6.21 mm at the maximum capacity. The total range in axial deformation ranged from 6.02 mm to 6.28 mm, with an average of 6.15 mm. The differences in axial deformation was relatively small, ΔU_x=0.26 mm, or about 4.23% of the average. The most severe lateral deflection of the plate at the limit state was approximately 9 mm. The node that had most lateral deflection, which is also marked in Section 7.2, changed its lateral deflection from negative to positive. The change came approximately the same time as the panel reached its ultimate capacity, Its z-deflection change in the LPF-arc length space was gradual. It did not snap rapidly.

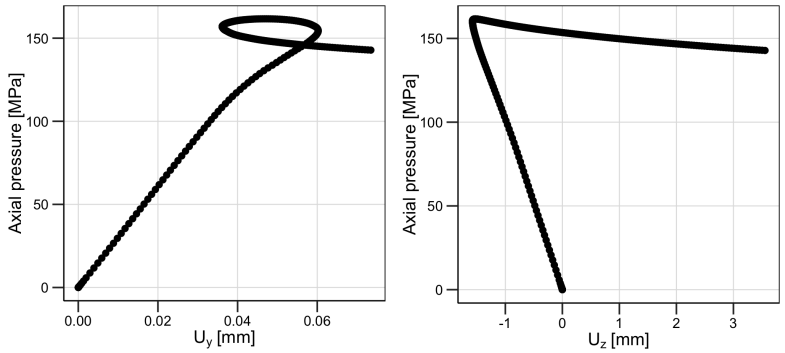

Figure 7.1: The Uy and Uz movement of the node that had largest lateral deformation for P6-WF8-T8. Note how the change in Uz coincides with ULS.

7.1.2 Abaqus - Change of HAZ Patterns

Changing the HAZ patterns had a significant effect on the ultimate axial capacity. The least significant change, was removing the HAZ from the plate-girder connection. Surprisingly it lead to a decreased ultimate capacity of 0.22%. Adding more HAZ to the web-girder connection also decreased the ultimate capacity. It was decreased by 1.05%. Not having HAZ on the plate and not having HAZ at all resulted in an increased ultimate axial capacity of 11.88% and 19.19% respectively.

7.1.3 Change of Poisson's Ratio

During the review phase of the project, it was discovered that *Eurocode 9* uses a Poisson's ratio of 0.3, while *RU-HSLC* uses a Poisson's ratio of 0.33. Thus the ratio is 10% higher in *RU-HSLC*. The Abaqus analysis was performed using 0.3 as Poisson's ratio. Changing the ratio from 0.3 to 0.33 had a slight effect of 0.18% increased ultimate axial strength.

Table 7.1: Results from Abaqua Riks-analysis of the ultimate strength of stiffened aluminium panels in uniform axial compression. σ_{ULS} denotes the maximum achieved load pressure and U_x denotes the axial deformation of the plate edge at that point. $\%\Delta\sigma_{ULS}$ denotes the percentage change of σ_{ULS} relative to the base case P6-SF8-T10 and $\%\Delta A$ denoted the percentage change of the cross sectional area relative to the base case (only stiffener and plate). ΔA refers to the area that have been changed. The name Px-SFy-Tz refers to a panel with dimensions t_P=x mm, t_W=t_F=y mm and t_T=z mm.

Panel Type	U_x **[mm]**	σ_{ULT} **[MPa]**	$\%\Delta\sigma_{ULT}$	$\%\Delta A$
P6-WF8-T10	6.2183	161.65		
P7-WF8-T10	6.2801	170.74	+ 5.62	+11.17
P6-WF5-T10	6.0125	152.06	- 5.93	-11.64
P6-WF6-T10	6.0690	155.44	- 3.84	-7.82
P6-WF7-T10	6.1274	158.66	- 1.85	-3.88
P6-WF8-T8	6.1720	161.32	- 0.21	
P6-WF8-T9	6.1849	161.50	- 0.095	
HAZ pattern modifications	U_x **[mm]**	σ_{ULS} **[MPa]**	$\%\Delta\sigma_{ULS}$	ΔA **[m^2]**
Base case: P6-WF8-T10	6.2183	161.65		
HAZ removed from long plate edges	6.3732	167.75	+ 3.77	0.112
HAZ removed from plate-girder connection	6.1771	161.30	- 0.22	0.100
HAZ added to stiffener-girder connection	6.1300	159.96	- 1.05	0.167
Without HAZ on plate	6.5532	180.86	+ 11.88	0.561
Without HAZ on plate and stiffener	6.4848	192.67	+ 19.19	0.734
Change of Poisson's Ratio	U_x **[mm]**	σ_{ULT} **[MPa]**	$\%\Delta\sigma_{ULT}$	
Basecase: P6-WF8-T10	6.2183	161.65		
ν changed from 0.3 to 0.33	6.1784	161.95	+ 0.18	

7.2 Results table

7.2.1 Correlation of Area and ULS

As expected the axial ultimate limit state capacity increases with increased cross-sectional area. In Section 7.2.1 the combined cross-sectional area of the stiffener and plate are plotted versus the axial ULS pressure, for P6-WF5-T10 to P6-WF8-T10 and for P7-SF8-T10. Six and five significant numbers where used for the ULS and area, respectively. First, normality was confirmed through the Shaprio-Wilk normality test. Then correlation was calculated using the cor.test() function that confirmed that the variables stress and area indeed were positively correlated with a Pearson correlation coefficient of 0.9999511 (t-test significance value 4.11e-07). The Pearson correlation test was applied in R.

7.3 Eurocode 9 Results

The results of the *Eurocode 9* analysis are listed in Table 7.2. As expected the the strength decreases when the web is considered an external part because it is then defined as cross-section class 4, i.e. the cross-section must be reduced due to local buckling. For panels with equal web and flange thickness, the average reduction was 6.34 MPa.
In Table 7.4 the multi-stiffened *EC9* panel is compared with similar results of the Abaqus analysis. The results of *EC9* was approximately 2.1-2.9 % lower than the results from the Abaqus analysis.

HAZ extent of 20 mm

For panels with an average web and plate thickness below 6 mm (and not to large difference in relative magnitude), the extent of the HAZ could be reduced to 20 mm. The effect of this reduction is listed in Section 6.2.

Internal or outstand web

The buckling resistances of the panel where also calculated with the assumption that the web was an outstand. The most important effect was that it was then classified as an cross-section class 4 part, and thus its thickness had to be reduced.

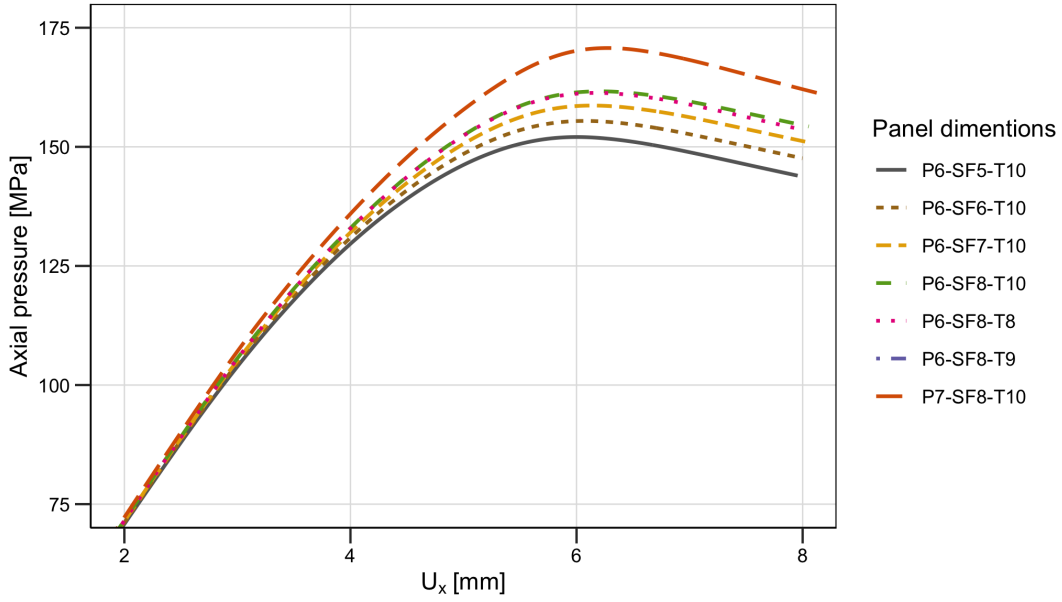

Figure 7.2: Panels with different dimensions. The applied axial load pressure during Riks analysis and associated axial deformations of the straight load edge.

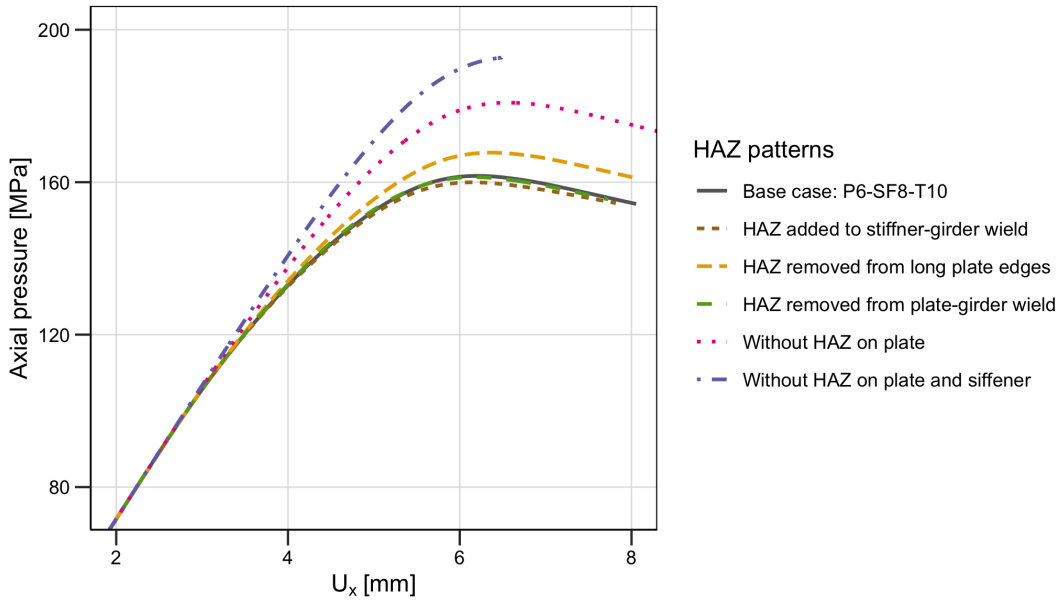

Figure 7.3: Panels with different HAZ patterns. The applied axial load pressure during Riks analysis and associated axial deformations of the straight load edge.

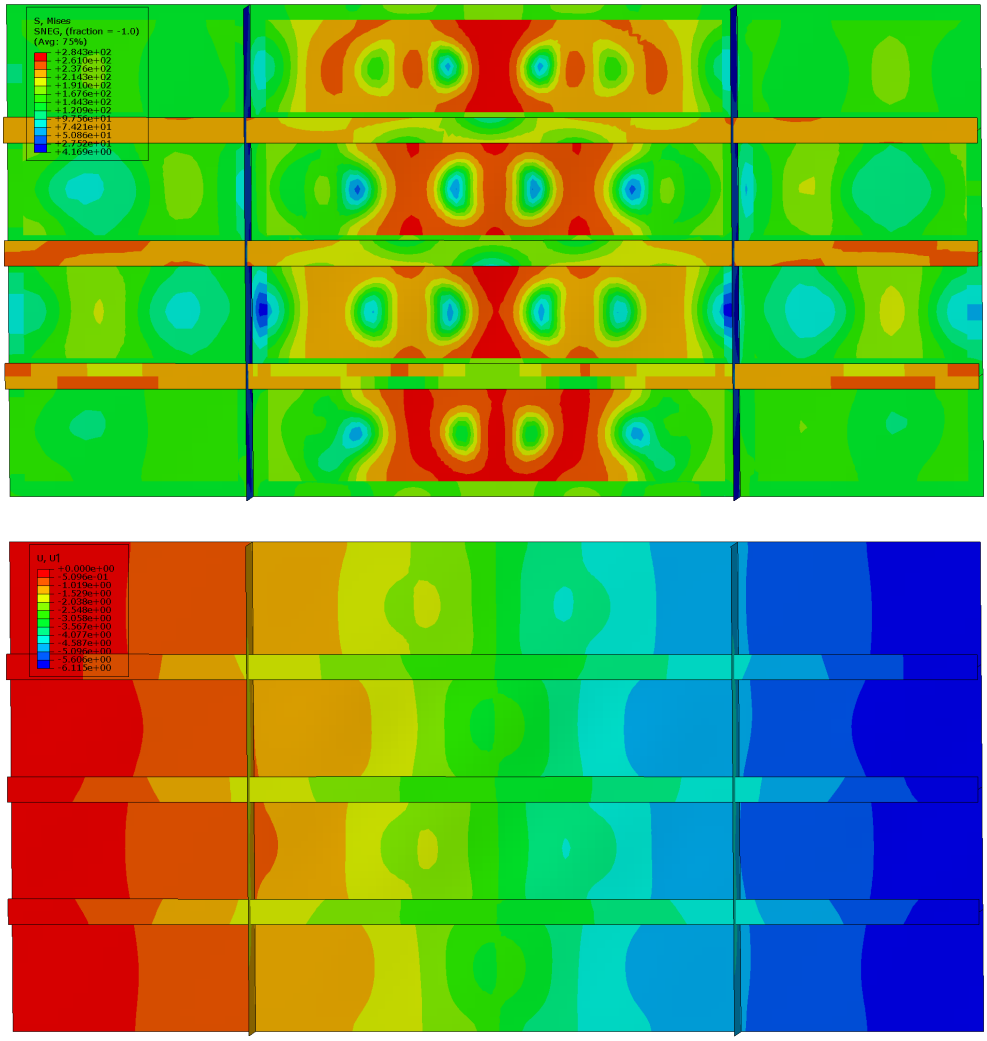

Figure 7.4: Panel P6-SF8-T10 at the point of maximum capacity. Top: Mises stress. Bottom: Axial deformation.

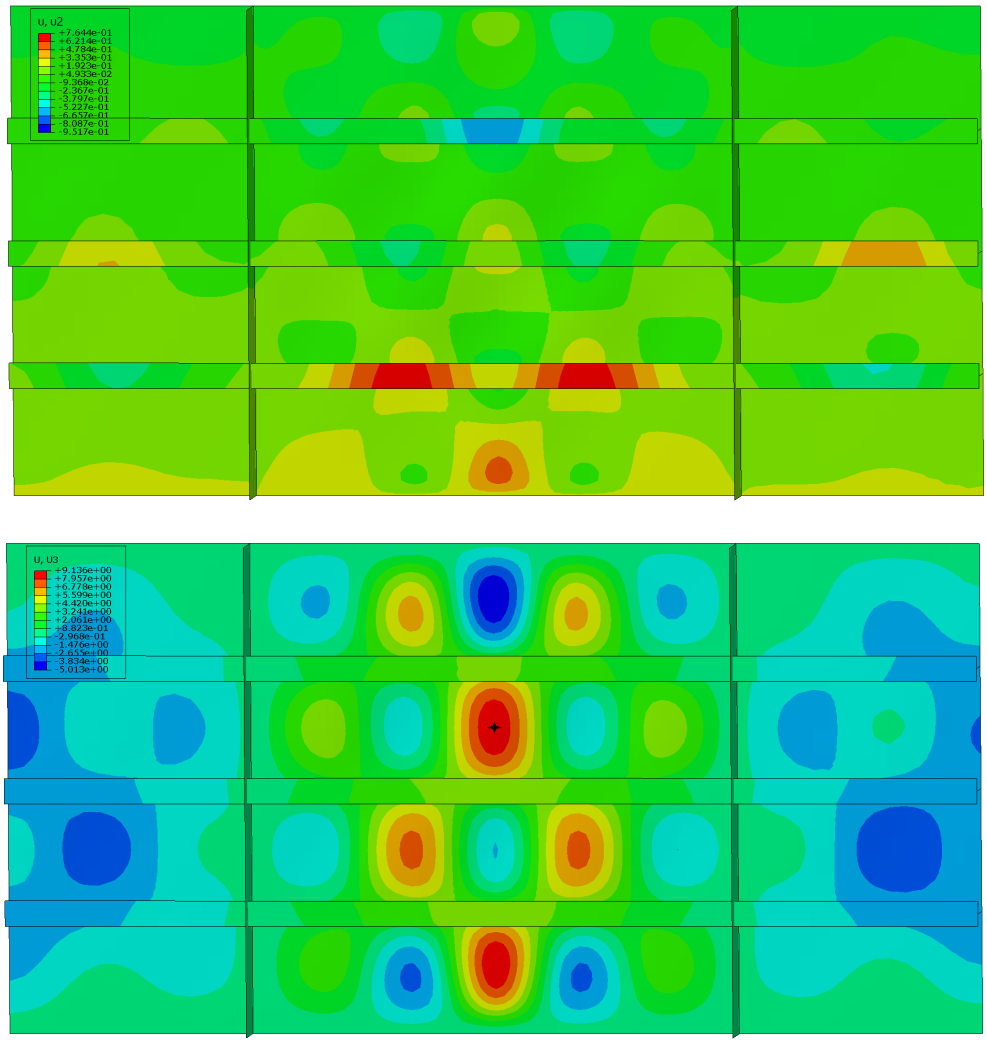

Figure 7.5: Panel P6-SF8-T10 at the point of maximum capacity. Top: Transverse deformation (y-direction). Bottom: Lateral deformation (z-direction). The black star marks the node that had largest lateral deformation.

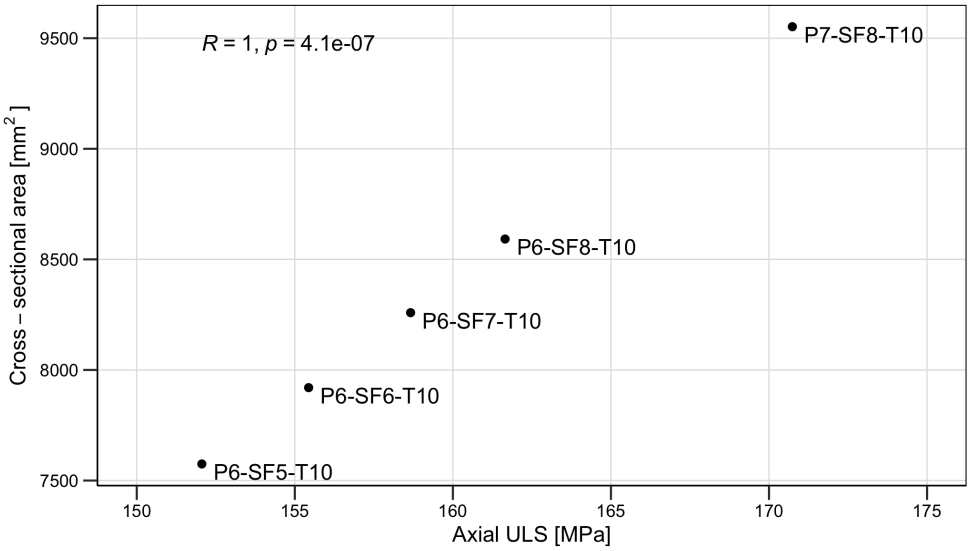

Figure 7.6: The combined cross-sectional area of the stiffener and plate correlates linearly with the axial ULS pressure load.

Table 7.2: Design resistance of panel with length 950 mm and 3 T-stiffeners according to EC9. Dimensions are similar as to in Chapter 6, but with only the panel part in between the girders.

Panel Type	**Multi-3 1)**	**Multi-3 2)**
P6-WF4	144.69	135.60
P6-WF5	148.93	140.42
P6-WF6	152.17	144.38
P6-WF7	154.81	148.10
P6-WF8	157.03	151.60
P6-WF9	158.92	154.85
P6-WF10	160.49	157.74
P6-W7-F8	156.41	150.1
P6-W6-F8	155.75	148.79
P6-W5-F8	155.05	147.74
P6-W4-F8	154.30	146.80
P6-W8-F4	149.97	142.93
P6-W8-F5	152.04	145.42
P6-W8-F6	153.88	147.66
P6-W8-F7	155.53	149.71
P6-W8-F8	157.03	151.60
P6-W8-F9	158.41	153.36
P6-W8-F10	159.69	155.00
P6-WF4*	146.31	135.38
P6-WF5*	150.95	140.38
P6-WF6*	154.52	144.80
P6-W6-F8*	158.07	19.29
P6-W5-F8*	157.04	147.82
P6-W4-F8*	155.93	146.64
1) The web is considered an internal part.		
2) The web is considered an external part.		
* HAZ extent was reduced to 20 mm.		

Table 7.3: Design Resistance of plate with dimensions 232 mm x 950 mm. The dimensions are smaller than the regular panel because the thicknesses $t_w = 8$mm and t_g =10 mm are subtracted.

Plate Thickness	**Plate**
3	85.47
4	110.29
5	133.26
6	154.39
7	168.85
8	181.79
9	193.37

Table 7.4: Design resistance of panel with length 950 mm and 3 T-stiffeners according to EC9. Stiffened panel analysed with Abaqus. Reduction of EC9 relative to Abaqus result.

Panel Type	**Multi-3 1)**	**Abaqus**	**%-ULS**
P6-WF5-T10	148.93	152.06	2.06
P6-WF6-T10	152.17	155.44	2.10
P6-WF7-T10	154.81	158.66	2.43
P6-WF8-T10	157.03	161.65	2.86
1) The web is considered an internal part.			

Table 7.5: Design resistance of panel with length 950 mm and 3 T-stiffeners according to EC9. Note that 2) stresses are lower because the web is considered slender and is reduced due to local buckling.

Panel Type	**Multi-3 1)**	**Multi-3 2)**	**%-diff)**
P6-WF4	144.69	146.31	1.12
P6-WF5	148.93	150.95	1.36
P6-WF6	152.17	154.52	1.54
P6-W6-F8	155.75	158.07	1.49
P6-W5-F8	155.05	157.04	1.28
P6-W4-F8	154.30	155.93	1.06
1) The web is considered an internal part. 1) The web is considered an outstand part.			

Chapter 8

Discussion

8.0.1 Abaqus Results versus Eurocode 9

Four panel types are compared in Table 7.4. The results from Eurocode where only 2.1-2.9% lower than the results from Abaqus. This shows that the FEA analysis was modelled adequately. It is also a good sign that the *Eurocode 9* results where lower than the Abaqus results as they are supposed to be slightly on the conservative side.

8.1 Changing the HAZ Pattern

This study has reaffirmed that modelling the heat affected material properties of aluminium has significant effect on the ultimate axial capacity. When the buckling strength of slender structures are assessed with *Eurocode 9*, it is allowed to neglect heat affected zones that are transverse to the loading direction and that have lateral restraint. The heat affected Zone on the plate-girder connection fits those requirements and the FEM results support those assessments. However, the heat affected zones on the stiffener-girder connection also fits the same criteria, but modelling it with or without HAZ did have an 1% impact. On the other hand, *Eurocode 9* takes some of those simplifications into account by using safety factors and conservative assumptions elsewhere.

8.1.1 Change of Poisson's Ratio

As stated in the results the Poisson's ratio was altered in one run(base case P6-WF8-T10) to check its effects. It was originally 0.3, which is in accordance with *EC9*, and changed to 0.33, which is in accordance with *RU-HSLC*. The change resulted in a slightly increased ultimate axial strength. For comparison, the elastic buckling strength has the term $\frac{1}{(1-\nu^2)}$. Thus the naive expected change may be formulated as $\frac{\sigma_{E,0.33}}{\sigma_{E,0.3}} = \frac{(1-0.3^2)}{(1-0.33^2)} = 1.02120$, thus a 2.12% change. The difference in FEA ultimate axial capacity was only 0.18%, or only 0.3 MPa. These values can however

not be compared directly. The result of the elastic buckling formula is a theoretic limit state, but buckling usually occurs much earlier.

8.1.2 Unstiffened Panel Model

For reasons of comparison, the ultimate resistance capacity of the panel may also be estimated by the ultimate capacity of an unstiffened plate. The plate has a width of 232 mm and a length 950 mm. That corresponds to a panel with stiffener web thicknesses of 8 mm and transverse girder thicknesses of 10 mm. The results are listed in Table 7.3. The unstiffened plate with a thickness of 6 mm had an ULS of 154.39 MPa, which is quite similar to the Abaqus panel P6-WF6-T10, which was at 155.44 MPa. The ULS of Abaqus P6-WFxx-T10 panels ranges from 158.66 MPa to 161.65 MPa. This suggests that the ULS of the panel is dominated by buckling in the plate, and that the stiffeners are relatively strong. The weakness of the plate relative to the stiffeners was also seen by the deformations. In general the plate deforms more much more than the stiffeners.

An interesting difference between the unstiffened panel model and the Abaqus model is the boundary conditions. The unstiffened panel model may be used with boundary conditions that are less restraining than those in the Abaqus model. The panel may for instance have a hinged support or even be free along one longitudinal edge.

8.1.3 Correlation between Area and ULS

As stated in Section 7.2.1, a linear correlation between the panel cross-section and ultimate buckling strength capacity. The correlation is very high, but its not clear if the correlation can be trusted to be as linear as the plot and Pearson coefficient (=0.9999511) suggests. The input parameter where for instance rounded, but on the other hand 5 and 6 significant numbers is quite good. It is less strange that there was a linear relation for the panels with plate thickness of 6 mm. For those panels, the area increment was constant. The panel P7-WF8-T10 did however change in a qualitatively different way than the other, and thus its strange that it would lie on a perfect line with the others.

The smaller panel

The model was originally meant to have five stiffeners and be a three-span model, but it was simplified in order to make it computationally easier to analyse. As described in **??**, the original plan was to model a plate with similar a and b values, but with 3 girders and 5 stiffeners. That panel would cover an area approximately 2.2 times as big as the panel that was chosen. A buckling eigenvalue analysis was however performed on the larger model. With all other conditions equal, the eigenvalue of the bigger model was about 3.2% lower. Thus, there the theoretical buckling capacity increased with 3.2%, but its unclear whether the ultimate capacity

would increase equally. Keep in mind, that the eigenvalue analysis only takes linear material behavior into account.

Girders

The girders were modelled to be approximately half as tall one could expect from similar real-world aluminium hulls. The reason for this choice was to reduce the computational cost, and the toll on the accuracy was determined to be negligible for the following reasons. The panel model was built to test the axial capacity and did therefore not have any z-direction loads. The purpose of the girders were therefore not to carry external loads, but to add realistic stiffness to the plate and stiffener web. In addition the stiffener top was only restricted to not move in the z-direction and to not rotate about the z-axis. The effects of these boundary conditions on the web and plate would be minuscule if the girder height were to be changed.
For reasons of simplicity, the girders were also not modeled with any heat affected zones. This could also slightly reduce the computational cost. It was however observed, that the stress level in the girder never rose above the linear range of any of the material-descriptions. Thus modelling the girders with 5083-H24 or with 6082-T6 and with or without HAZ would not make any difference.

Slider on the long plate edges

The long plate edges were forced to remain straight, but the edge line was allowed to rotate about the z-axis as a straight line and move in the x- and y- direction as a straight line. Due to the high resistance of the transverse girders, the edge line did not rotate. Therefore, the same behaviour could have been achieved by restricting the long edges to not move in the z-direction, to not rotate about the x-axis and to force the nodes on the line to move together in the y-direction (with the equation constraint).

8.2 Potential Sources of Modelling Errors

The extra boundary condition to the stiffener edges

As explained in Section 6.4 the stiffener ends were restricted to not rotate about the x-axis, effectively eliminating the torsional rotation of the ends. This choice added some extra torsional rigidity to the whole structure and therefore the model may not be conservative for torsional buckling analysis. On the other hand, the stiffeners were forced to rotate with the girders, and it may be that the part of the stiffeners between the girders, would respond quite similarly without the extra boundary condition. In addition, the flange elements where only partly tied to the girder elements. That is, only the middle node (shared with the web) was tied to

follow the movement and rotation of the girder. In many similar real world panels, the flanges are often welded to the girder.

Shear Locking and hourglass modes

There are several phenomenons that can cause excessive, unrealistic stiffness to a finite element analysis. Two of those are shear locking and hourglass modes. As described in Section 5.4.1, the chosen S4R elements are not prone to shear locking nor hourglass modes.

Material Data

According to Chen [23], the stress-strain relationship between the elastic limit and the 0.2% proof stress has significant effects on the axial capacity of aluminium plates and panels, but the part above the 0.2% proof stress has small effect. Since the material behaviour above the elastic range is implemented into the model with discrete stress-strain data points with linear relation between two consecutive pairs, the number of data points will affect the results. The number of data points chosen, is a trade off decision between accuracy and computational cost. I did not find any recommendations on the number of data points. The materials were modelled with about 20 to 30 data points. A plot in Excel was used to visualize the curve, and I focused on having many data points at the most curved part of the stress strain curve, and fewer at the early semi-linear phase and after the 0.2% proof stress. The true stress strain curves are plotted in Section 6.2.

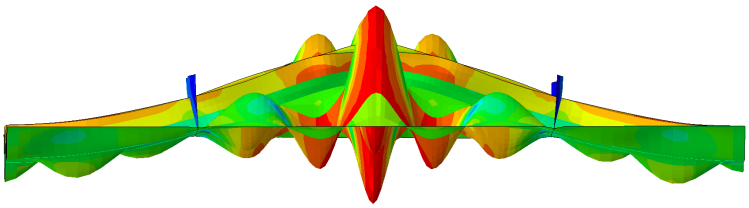

Figure 8.1: The P6-WF8-T10 at maximum resistance capacity. Deformations are scaled 30x.

Chapter 9

Conclusion

The estimated ultimate buckling strength of the Abaqus analysis corresponds well with expected values obtained through *Eurocode 9* formulations. The physical assumptions and implementations of the model was therefore quite realistic.
The study reaffirms that the heat affected zones have a significant influence on the ultimate buckling strength of stiffened aluminium panels. The study also reaffirms the *EC 9* assumption that transverse welds with lateral support may be ignored, but only if they are on the plate. Heat affected zones on the web-girder connections should be implemented into the model, unless significant margins and safety factors are applied elsewhere.

Bibliography

[1] *Design of aluminium structures, introduction to eurocode 9 with worked examples*, PDF, Nov. 2020.

[2] S. Misra, *Design Principles of Ships and Marine Structures*, eng. Taylor Francis Group, 2016, ISBN: 978-1-4822-5447-1.

[3] S. Ferraris and L. M. Volponis, 'Aluminium alloys in third millennium shipbuilding: Materials, technologies, perspectives,' eng, *The Fifth International Forum on Aluminum Ships*, p. 11, 2005.

[4] P. Sensharma, M. Collette and J. Harrington, *Effect of welded properties on aluminum structures, ssc-460*, 2010.

[5] J. Kissel and R. L. Ferry, *A Guide to Their Specifications and Design, Second Edition*, eng. John Wiley Sons, 2002, ISBN: 0-471-01965-8.

[6] J. e. A. Mish Wh, *High speed aluminum vessels design guide, ssc-464*, 2012.

[7] D. GL, *Dnvgl-ru-ship, ships*, `https://rules.dnvgl.com/ServiceDocuments/dnvgl/#!/industry/1/Maritime`, 2020.

[8] D. Kopeliovich, *Substech*, `https://www.substech.com/dokuwiki/doku.php?id=aluminum_alloys`, 2012.

[9] E. Byklum, *Ultimate strength analysis of stiffened steel and aluminium panels using semi-analytical methods*, Phd Thesis, 2002.

[10] J. K. Paik and O. F. Hughes, *SHIP STRUCTURAL ANALYSIS AND DESIGN*, eng. The Society of Naval Architects and Marine Engineers, 2010, ISBN: 978-0-939773-78-3.

[11] R. Sielski, *Aluminum structure design and fabrication guide, ssc-452*, 2007.

[12] O. H. H. Kristensen, 'Ultimate capacity of aluminium plates under multiple loads, considering haz properties,' Ph.D. dissertation, Norwegian University of Science and Technology, 2001.

[13] Y. Zha and T. Moan, 'Experimental and numerical study of torsional buckling of stiffeners in aluminium panels,' eng, *Journal of Structural Engineering*, vol. 129, no. 2, pp. 160–165, 2003.

[14] Y. Zha and T. Moan, 'Ultimate strength of stiffened aluminium panels with predominantly torsional failure modes,' eng, *Thin-Walled Structures*, vol. 39, no. 8, pp. 631–648, Aug. 2001.

[15] J. Amdahl, *Tmr4205 buckling and ultimate strength of marine structures*, 2020.

[16] I. Habibi, Triyono and N. Muhayat, 'A review on aluminum arc welding and it's problems,' eng, *Proceedings of the 6th International Conference and Exhibition on Sustainable Energy and Advanced Materials*, vol. 6, pp. 819–826, 2019.

[17] V. Farajkhah, Y. Liu and L. Gannon, 'Finite element study of 3d simulated welding effect in aluminium plates,' eng, *Ships and Offshore Structures*, vol. 12, pp. 196–208, 2016, ISSN: 1744-5302.

[18] W. Ramberg and W. Osgood, *Description of stress–strain curves by three parameters*, Technical Note No. 902, 1943.

[19] S. P. Timoshenko and J. M. Gere, *Theory of Elastic Stability*, eng. McGraw Hill, 1963, ISBN: 07-Y85821-7.

[20] J. K. Paik and B. J. Kim, 'Ultimate strength formulations for stiffened panels under combined axial load, in-plane bending and lateral pressure: A benchmark study,' eng, *Thin-Walled Structures*, vol. 40, pp. 45–83, 2001, ISSN: 0263-8231.

[21] M. Haugen, *Non-linear buckling analysis for ultimate limit strength calculations of doubler plate repair on a damaged ship structure*, Sep. 2012.

[22] *Abaqus documentation*, 6.6, 2020. [Online]. Available: `https://abaqus-docs.mit.edu/2017/English/SIMACAEEXCRefMap/simaexc-c-docproc.htm`.

[23] Q. Chen, 'Ultimate strength of aluminium panels, considering haz effects,' Ph.D. dissertation, Norwegian University of Science and Technology, Sep. 2011.

[24] N. Vasios, *The arc length method*, `https://scholar.harvard.edu/files/vasios/files/ArcLength.pdf`, 2020.

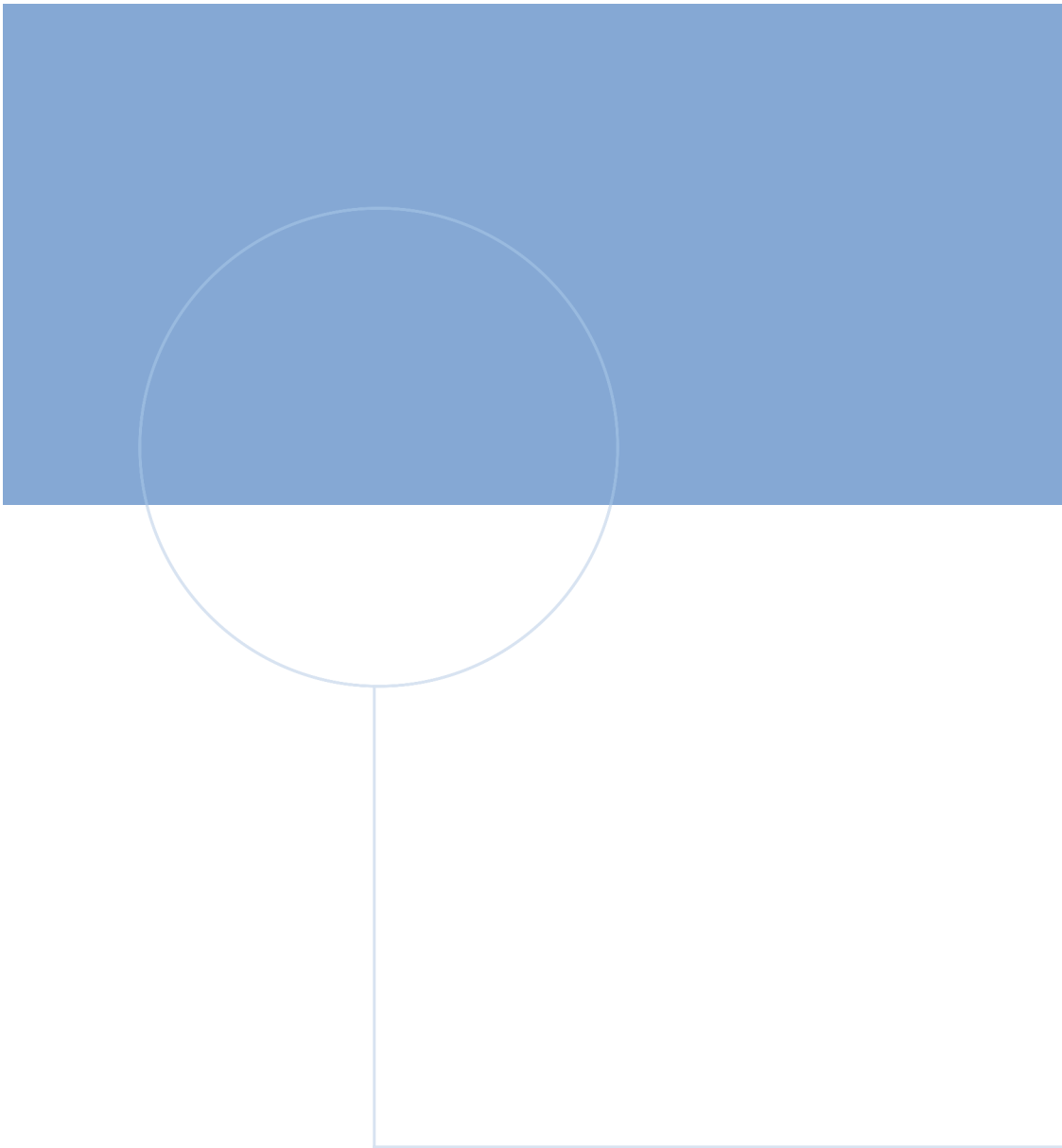

NTNU

Kunnskap for en bedre verden